The physical law governing the movement must be valid for any (angular) velocity $\frac{d\alpha}{dt}$, thus we can divide by $\frac{d\alpha}{dt}$ to get at:

$$m\ell^2 \frac{d^2\alpha}{dt^2} + mg\ell \sin\alpha = -F\ell\sin\alpha$$

$$\Downarrow$$

$$\frac{d^2\alpha}{dt^2} = -\frac{g}{\ell}\sin\alpha - \frac{F}{m\ell}\sin\alpha. \tag{6.2}$$

The pendulum model in Eq. 6.2 can be rewritten in state space form as

$$\frac{d\alpha}{dt} = \omega \tag{6.3}$$

$$\frac{d\omega}{dt} = -\frac{g}{\ell}\sin\alpha + \frac{F}{m\ell}\sin\alpha \tag{6.4}$$

where g is a natural constant, m, ℓ are parameters, F is a variable input, while α, ω are states. ▲

6.2.5.2   Multi-body, one degree of freedom*

...under construction...

6.2.5.3 n degrees of freedom*

...under construction...

6.2.5.4   Energy balance vs momentum balance*

...under construction...

6.2.6   Lagrangian mechanics$^{\star,+}$

...under construction...

6.2.7   Beams, torsion$^{\star,+}$

...under construction...

6.3   Spatial description

6.3.1   Momentum balance

We have seen that for a closed system/material description, Newton's law is equivalent to the linear momentum balance

$$\frac{d\mathcal{M}}{dt} = F.$$

We are now interested in extending the momentum balance to the case of a spatial description, where we allow for mass to flow into and out of the system. The extension is straightforward, and the general momentum balance becomes

$$\frac{d\mathcal{M}}{dt} = \dot{\mathcal{M}}_\text{i} - \dot{\mathcal{M}}_\text{e} + F. \tag{6.5}$$

As we have seen, the momentum is

$$\mathcal{M} = mv, \tag{6.6}$$

where m is the (possibly varying) mass and v is the linear velocity. The linear velocity v is an intensive variable, while the mass is an extensive variable. It follows that the momentum flowing with matter is given as

$$\dot{\mathcal{M}} = \dot{m}v, \tag{6.7}$$

where $\dot{m}$ is the mass flow rate.

The simple formulation above is valid when the velocity vector v is perpendicular to the surface ∂V through which it flows; $v \perp \partial V$. In a more general case, we can write

$$\dot{\mathcal{M}}_\text{i} - \dot{\mathcal{M}}_\text{e} = -\oint_{\partial V} \rho v \cdot v^T n \cdot dA$$

where ∂V is the surface of the system and n is the outwardly pointing normal vector to the surface. However, in these notes, we will use the simple formulation where $\dot{\mathcal{M}} = \dot{m}v$.

Some of the force terms F relate to forces operating on the boundary ∂V of the system, e.g., pressure forces. Other force terms operate within the system volume V, e.g., gravity, friction, etc. The forces operating within the system volume V are considered as source terms in the balance law, hence the momentum balance is strictly speaking not a conservation law as defined in these notes.

Similarly, we can introduce an angular momentum balance in a spatial description, which takes the form

$$\frac{d\mathcal{A}}{dt} = \dot{\mathcal{A}}_\text{i} - \dot{\mathcal{A}}_\text{e} + T \tag{6.8}$$

where the angular momentum is

$$\mathcal{A} = J\omega \tag{6.9}$$

Here, if the material influent is given at a fixed radius and tangential to the radius, we have

$$\dot{\mathcal{A}} = r \cdot \dot{\mathcal{M}}. \tag{6.10}$$

6.3.2   Mechanical energy balance

We have seen that in the material description, the mechanical energy balance can be written as in Eq. 6.1:

$$\frac{dE}{dt} = \dot{W},$$

where energy E is the sum of kinetic and potential energy, $E = K + P$, and where kinetic energy K can come from linear movement, $K = \frac{1}{2}mv^2$, or angular movement, $K = \frac{1}{2}J\omega^2$, while the work rate is related to generalized force multiplied by generalized velocity: $\dot{W} = Fv$ for linear movement and $\dot{W} = T\omega$ for angular movement. Potential energy P describes the potential of those conservative forces that are not included in the work rate term $\dot{W}$.

In a spatial description, we need to include the possibility of a change of mass within the system boundaries as well flow of energy transported by mass flow. Thus, the mechanical energy balance changes to

$$\frac{dE}{dt} = \dot{E}_\mathrm{i} - \dot{E}_\mathrm{e} + \dot{W} \tag{6.11}$$

where $\dot{E} = \dot{K} + \dot{P}$. By comparing the expression for linear kinetic energy $K = \frac{1}{2}mv^2$, we can express kinetic energy flow rate as

$$\dot{K} = \frac{1}{2}\dot{m}v^2 = \frac{1}{2}\dot{m}v \cdot v = \frac{1}{2}\dot{\mathcal{M}}v.$$

Similarly, we could have a potential energy, say $P = mgz$, with potential energy flow rate $\dot{P} = \dot{m}gz$. In both cases, it is an underlying assumption that the mass flow $\dot{m}$ enters the system. If the mass flow rate $\dot{m}$ instead hits the system boundary and creates a force F working on the system, this effect should be included in the work term as $\dot{W} = Fv$.

Similarly, for angular movement, the kinetic energy $K = \frac{1}{2}J\omega^2 = \frac{1}{2}\mathcal{A}\omega$ should give rise to a convective kinetic energy flow rate as

$$\dot{K} = \frac{1}{2}\dot{\mathcal{A}}\omega. \tag{6.12}$$

Here,

$$\dot{\mathcal{A}} = r\dot{\mathcal{M}} = r\dot{m}v.$$

Similary, we could envision a potential energy flow $\dot{P}$. Again, it is an underlying assumption that the mass flow $\dot{m}$ enters the system.

The mechanical energy balance for angular movement is commonly used for turbo machines. In that case, a fluid moving with mass flow rate $\dot{m}$ hits blades of an object rotating with angular velocity ω. However, the fluid mass does not become part of the rotating mass, hence for turbo machines, $\dot{K} \equiv 0$, and normally the level difference $z_\mathrm{i} - z_\mathrm{e}$ is so small that we can neglect $\dot{P}$. Furthermore, the moving fluid hits (or leaves) the blades of the rotating mass at a radius r with a torque $T = \dot{\mathcal{A}} = r\dot{\mathcal{M}}^\mathrm{t}$ where $\dot{\mathcal{M}}^\mathrm{t}$ is the projection of momentum flow rate of the moving fluid, $\dot{\mathcal{M}} = \dot{m}v$, on the direction *tangential* to the rotation. Thus, $\dot{\mathcal{M}}^\mathrm{t} = \dot{m}v^\mathrm{t}$ — where it has been assumed that the mass flow rate $\dot{m}$ actually is tangential to the rotation and parallel to v, but where subscript t has been added to v^t for clarity. The resulting work rate is $\dot{W} = T\omega$. Introducing the "reference" velocity of the rotating object at the "point of attack", $v_\rho = r\omega$, the work rate can be written as

$$\dot{W} = T\omega = \omega r \cdot \dot{\mathcal{M}}^\mathrm{t} = v_\rho \cdot \dot{m}v^\mathrm{t}. \tag{6.13}$$

As stated above, v_ρ is the reference velocity of the rotating object (the turbine mass, etc.), while $\dot{m}$ and v^t refer to the flow of the fluid hitting (or leaving) the rotating object.

6.4   Friction

6.4.1   Friction and pressure drop in filled pipes

6.4.1.1   Overview of friction force

The friction force F_{f} is directed in the opposite direction of the velocity v of the fluid. A common expression for friction force in filled pipes is the following:

$$F_{\mathrm{f}} = K'''A_{\mathrm{w}}f. \tag{6.14}$$

In Eq. 6.14, K''' is the kinetic energy per volume,

$$K''' = \frac{1}{2}\rho \langle v \rangle^2$$

where ρ is density and $\langle v \rangle$ is the linear velocity average across the cross-section of the pipe. Furthermore, in Eq. 6.14, A_{w} is the wetting surface, i.e., the contact surface between the fluid and the wall; $A_{\mathrm{w}} = \wp L$ where $\wp$ is the perimeter of the pipe — $\wp = \pi D$ for a circular pipe. Finally, in Eq. 6.14, f is Fanning's friction factor.

Clearly, Eq. 6.14 does not include direction of vectors in the expression. If we would include the direction of F_{f} and the direction of the velocity, a more correct expression would be

$$F_{\mathrm{f}} = -K'''A_{\mathrm{w}}f$$

with

$$K''' = \frac{1}{2}\rho \langle v \rangle \cdot |\langle v \rangle| . \tag{6.15}$$

It is common to use the more readable expression in Eq. 6.14, and include an understanding of the correct direction of friction force vs. velocity in the model development. Still, care must be shown if the flow changes direction; in that case the expression for K''' in Eq. 6.15 must be used.

The so-called Moody diagram depicts the friction factor f as a function of Reynolds' number, with the roughness ratio $\frac{\epsilon}{D}$ as parameter, see Fig. 6.6.

In Fig. 6.6, the *turbulent* region ($N_{\mathrm{Re}} > 2.3 \times 10^3$) is a flow regime where the velocity across the pipe has a *stochastic* nature, and where the velocity v is more or less uniform across the pipe when we average the velocity over some short time period. von Kármáns "law of the wall", see subsequent more detailed discussion and Eq. 6.25, gives a velocity profile which is relatively flat over a large fraction of the cross sectional pipe area.[2] The *laminar* region ($N_{\mathrm{Re}} < 2.1 \times 10^3$) is a flow regime with a regular velocity v which varies as a parabola with the radius of the pipe, with zero velocity at the pipe wall and maximal velocity at the center of the pipe.

As discussed above, Fanning's friction factor will vary with the roughness of the pipe surface, specified by roughness height ϵ. Table 6.1 indicates the roughness of some pipe materials.[3]

Some publications use Darcy's friction factor f_{D} instead of Fanning's friction factor f; these two friction factors are related as $f_{\mathrm{D}} = 4f$.

---

[2]See `https://en.wikipedia.org/wiki/Law_of_the_wall`.
[3]Selected values taken from `https://neutrium.net/fluid_flow/absolute-roughness/`.
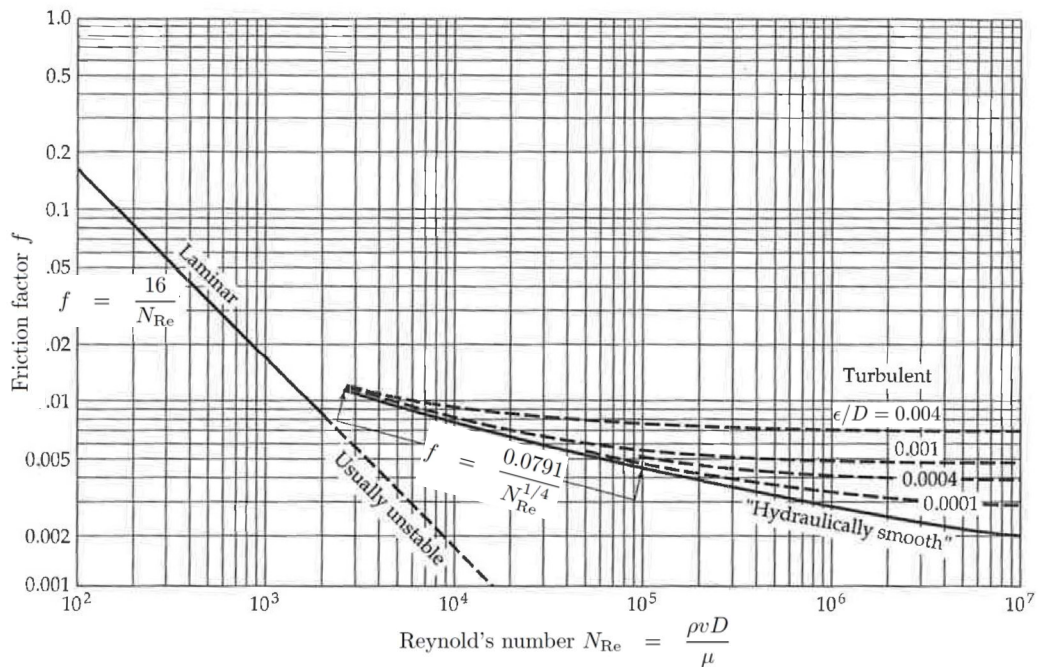
Figure 6.6: Moody diagram for Fanning's friction factor f for fluid flow in a pipe, as a function of the Reynolds number N_{Re}, Bird et al. (2002).

Table 6.1: Roughness height ϵ for various materials.

Material	Roughness ϵ, mm
Drawn tubing (glass, plastic)	$[0.0015, 0.01]$
Flexible rubber tubing (smooth)	$[0.006, 0.07]$
Stainless steel	0.03
Wrought iron (new)	0.045
Carbon steel (new)	$[0.02, 0.05]$
Carbon steel (slightly corroded)	$[0.05, 0.15]$
Carbon steel (moderately corroded)	$[0.15, 1]$
Carbon steel (badly corroded)	$[1, 3]$
Asphalted cast iron	$[0.1, 1]$
Galvanized iron	$[0.025, 0.15]$
Cast iron (new)	0.25
Concrete (very smooth)	$[0.025, 0.2]$
Concrete (fine, floated/brushed)	$[0.2, 0.8]$
Concrete (rough, form marks)	$[0.8, 3]$

6.4.1.2   Friction force and friction loss[+]

So far, we have treated the expression for the friction force F_f somewhat *ad hoc*.[4] Formally, friction force F_f directed in the opposite direction of the velocity v can be expressed as the product of shear stress τ_w between fluid and wall (force per area), and wall "wetting" surface A_w :

$$F_f = \tau_w A_w.$$

It follows that τ_w has the same direction as F_f. Shear stress τ_w is a function of the local velocity gradient of the fluid at the wall. For a straight, cylindrical pipe, the relevant gradient is the gradient in the radial direction, thus τ_w is a function of $\frac{\partial v}{\partial r}$: $\tau_w \left(\frac{\partial v}{\partial r} \right)$. For rigid walls, it is common to assume that the velocity at the wall is zero — this indicates that the velocity decreases when the radius approaches the wall, hence the gradient is negative at the wall and hence has the same direction as τ_w.

From thermodynamics, it can be shown that friction leads to a mechanical power "production" $\dot{W}_f$ given by

$$\dot{W}_f = -\tau_w \cdot \frac{\partial v}{\partial r}.$$

For *non-elastic* fluids, the functional relationship $\tau_w \left(\frac{\partial v}{\partial r} \right)$ is static. Then, the second law of thermodynamics (entropy production) dictates that $\dot{W}_f \leq 0$, in other words: friction leads to a loss of mechanical power[5] for non-elastic fluids.

It is straight forward to see that in general, function $\tau_w \left(\frac{\partial v}{\partial r} \right)$ must lie in the first and third quadrant of the coordinate system of $\left(\frac{\partial v}{\partial r}, \tau_w \right)$. The simplest possible choice of $\tau_w \left(\frac{\partial v}{\partial r} \right)$ that guarantees a negative $\dot{W}_f$, is

$$\tau_w = \mu \frac{\partial v}{\partial r} \tag{6.16}$$

leading to

$$\dot{W}_f = -\mu \left(\frac{\partial v}{\partial r} \right)^2 ;$$

here $\dot{W}_f$ is guaranteed to be negative (and thus produce entropy) provided that the proportionality factor $\mu > 0$. Quantity μ is known as (dynamic) *viscosity*, and the expression in Eq. 6.16 is known as Newton's shear stress law; fluids for which Newton's shear stress law is valid, are known as *Newtonian fluids*.

Some fluids show viscoelastic behavior, where there is a dynamic relationship for the shear stress, e.g., as in the Maxwell model:

$$\frac{d\tau_w}{dt} = \frac{1}{T_r} \left(-\tau_w - \mu \frac{\partial v}{\partial r} \right) ;$$

here, T_r is the relaxation time and μ is the viscosity. Realistic viscoelastic models may be considerably more complicated than the Maxwell model. Examples of

---

[4]*Ad hoc*: Latin expression, literally meaning "to this" (*ad* = to, *hoc* = this). The expression is used in the meaning "temporary", "informal", or "arranged for a particular purpose", as opposed to a "formal and general treatment". So far, we have used a temporary and simplified description of friction force (*ad hoc*); now it is time for a more general treatment.

[5]The lost mechanical power does not disappear: it leads to a heating of the fluid/wall.

viscoelastic fluids include, e.g., molten polymers. For viscoelastic fluids, the instantaneous friction power $\dot{W}_f$ may break the second law of thermodynamics during *transients* and may even become positive, but in *steady state* all systems must satisfy $\dot{W}_f \leq 0$.

6.4.1.3   Fanning friction[+]

Shear stress τ_w has dimension force/area or force-length/volume, which is work/volume or *energy/volume*. Studies in hydraulics have indicated that for a fully developed flow,[6] the shear stress τ_w between the fluid and the wall of a fixed object (e.g., a wall) is proportional to the kinetic energy of the fluid per volume, K'''; $\tau_w \propto K'''$. In 1877, Fanning[7] proposed the dimensionless friction factor/proportionality constant f,

$$f \triangleq \frac{\tau_w}{K'''},$$

known as Fanning's friction factor. Here, it must be observed that $f \geq 0$, i.e., we should really use the *absolute value* of the shear stress if we include directional information in its value. Assuming a Newtonian fluid, Fanning's friction factor f is a function of the so-called *Reynolds number* N_{Re}, Table 2.15 p. 36, here defined as:

$$N_{Re} = \frac{\rho \langle v \rangle D}{\mu};$$

here ρ is the fluid density, μ is the fluid viscosity, $\langle v \rangle$ is the average velocity of the fluid over a cross sectional area A,[8] and D is a characteristic dimension. Typically, D will be the diameter of the pipe if we are talking about friction against a pipe wall, while it may be the diameter of a sphere if we are talking about the drag force on a solid sphere "swimming" in the fluid flow; Bird et al. (2002). Observe that the Reynolds number N_{Re} is dimensionless.

If we express the friction force as $F_f = \tau_w A_w$, we find

$$f = \frac{\frac{F_f}{A_w}}{K'''}.$$
$$\Downarrow$$
$$F_f = K''' A_w f. \qquad (6.17)$$

In this friction law, K''' is defined as

$$K''' = \frac{\frac{1}{2}mv^2}{V} = \frac{1}{2}\rho v^2,$$

where ρ is the density of the fluid and v is the linear velocity of the fluid. If the fluid is allowed to reverse its direction of flow, the more general expression for K''' is

$$K''' = \frac{1}{2}\rho v \left| v \right|. \qquad (6.18)$$

At zero velocity, $v \rightarrow 0$, we will have $F_f \rightarrow 0$, since $K''' \rightarrow 0$ quadratically as $v \rightarrow 0$ while (as we will see) $f \rightarrow \infty$ linearly as $v \rightarrow 0$.

---

[6]"Fully developed" implies after the entrance effects have disappeared.

[7]John Thomas Fanning (1837–1911).

[8]Reynolds' number is positive, thus $\langle v \rangle$ is the numerical value (absolute value) of the velocity — in case the direction is included in the value of the velocity.
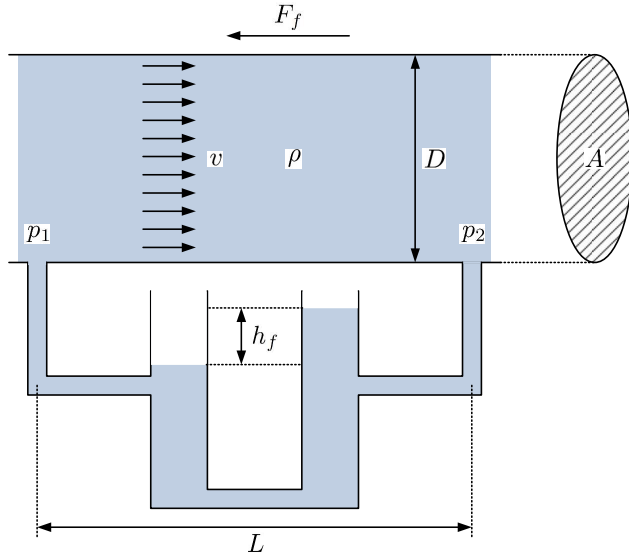
Figure 6.7: Measuring pressure drop $\Delta p_{\mathrm{f}} = p_1 - p_2$ due to friction, using a manometer.

6.4.1.4   Friction force and pressure drop[+]

Fanning introduced his friction factor in 1877. Figure 6.7 illustrates how the friction force is related to the pressure drop.

Assuming steady state conditions and constant density, the mass balance leads to

$$\frac{dm}{dt} = \dot{m}_1 - \dot{m}_2 \Rightarrow \dot{m}_1 = \dot{m}_2 \Rightarrow \dot{V}_1 = \dot{V}_2 = \dot{V} \Rightarrow v_1 = v_2 = v,$$

where the location of subscripts 1 and 2 are indicated in Fig. 6.7 for the pressures p_1 and p_2. The momentum balance is

$$\frac{d\mathcal{M}}{dt} = \dot{\mathcal{M}}_1 - \dot{\mathcal{M}}_2 + F.$$

In steady state, $\frac{d\mathcal{M}}{dt} = 0$, and $\dot{\mathcal{M}}_1 = \dot{\mathcal{M}}_2$ due to constant mass flow and constant density. The steady momentum balance thus only involves the pressure forces and the friction force, i.e.,

$$0 = p_1 A - p_2 A - F_{\mathrm{f}} \Rightarrow \Delta p_{\mathrm{f}} A = (p_1 - p_2)\, A = F_{\mathrm{f}}.$$

It follows that the pressure loss due to friction is

$$\Delta p_{\mathrm{f}} = \frac{1}{A} F_{\mathrm{f}} = \tau_{\mathrm{w}} \frac{A_{\mathrm{w}}}{A}.$$

6.4.1.5   Darcy friction[+]

Prior to Fanning's work, the pressure loss due to friction was expressed using the Darcy-Weisbach equation[9]

$$\frac{\Delta p_{\mathrm{f}}}{L} = f_{\mathrm{D}} \frac{\rho}{2} \frac{v^2}{D}. \tag{6.19}$$

_____

[9]Developed by Henry Darcy from the Prony equation of hydraulics, and further refined into the current form by Julius Weisbach in 1845.

How does the Darcy-Weisbach expression relate to Fanning's model?

Assuming a cylindrical pipe with diameter D, we find that $A_{\mathrm{w}} = \pi D L$, while $A = \pi \frac{D^2}{4}$. With $\tau_{\mathrm{w}} = K''' f$, Fanning's expression gives

$$\Delta p_{\mathrm{f}} = \frac{F_{\mathrm{f}}}{A} = \tau_{\mathrm{w}} \frac{A_{\mathrm{w}}}{A} = K''' f \frac{\pi D L}{\pi \frac{D^2}{4}} = 4 K''' f \frac{L}{D} L = 4 \frac{1}{2} \rho v^2 f \frac{L}{D}$$

$$\Downarrow$$

$$\frac{\Delta p_{\mathrm{f}}}{L} = 4 f \frac{\rho}{2} \frac{v^2}{D}. \tag{6.20}$$

Comparing Eqs. 6.19 and 6.20 gives

$$f_{\mathrm{D}} = 4f. \tag{6.21}$$

Because two different friction factors are used in the literature, it is important to know which friction factor is involved in the relevant friction factor model, and make sure that the correct factor is used in the chosen friction force expression.

6.4.1.6 Smooth pipe friction factors[+]

For laminar flow in a cylindrical pipe, it can be shown that the velocity has a parabolic profile over the radius, i.e.,

$$v(r) = v_{\mathrm{m}} \left(1 - \left(\frac{r}{R} \right)^2 \right)$$

where v_{m} is the maximal velocity found in the center, r is the distance from the pipe center, and R is the pipe radius. Laminar flow can be expected for $0 < N_{\mathrm{Re}} < 2.1 \times 10^3$, and it can be shown that with $N_{\mathrm{Re}} = \frac{\rho \langle v \rangle D}{\mu}$,

$$f_{\mathrm{D}} = \frac{64}{N_{\mathrm{Re}}} \Leftrightarrow f = \frac{16}{N_{\mathrm{Re}}}, \tag{6.22}$$

see Exercises 6.1 and 6.2.

For turbulent flow, $N_{\mathrm{Re}} > 2.3 \times 10^3$, it is common to rewrite the expression for the Darcy friction factor as

$$\frac{4}{f_{\mathrm{D}}} = \frac{K'''}{\tau_{\mathrm{w}}} = \frac{\frac{1}{2} \rho \langle v \rangle^2}{\tau_{\mathrm{w}}} \Rightarrow \frac{8}{f_{\mathrm{D}}} = \frac{\rho \langle v \rangle^2}{\tau_{\mathrm{w}}}$$

or

$$\sqrt{\frac{8}{f_{\mathrm{D}}}} = \frac{\langle v \rangle}{\sqrt{\tau_{\mathrm{w}}/\rho}} = \frac{\langle v \rangle}{v_\tau}.$$

Here, $v_\tau = \sqrt{\tau_{\mathrm{w}}/\rho}$ is known as the *shear velocity* or *friction velocity*. By observing that Reynolds' number $N_{\mathrm{Re}} = \frac{\rho \langle v \rangle D}{\mu}$ is dimensionless, it follows that $\frac{\mu}{\rho \langle v \rangle}$ has unit *length* and thus also $\frac{\mu}{\rho v_\tau}$ has unit length. We can then introduce some dimensionless

quantities:

$$v^* \triangleq \frac{v}{v_\tau}$$

$$R^* \triangleq \frac{R}{\frac{\mu}{\rho v_\tau}} = \frac{\frac{D}{2}}{\frac{\mu}{\rho v_\tau}} = \frac{\rho \langle v \rangle D}{\mu} \cdot \frac{v_\tau}{2 \langle v \rangle} = \frac{N_{\text{Re}}}{2} \frac{v_\tau}{\langle v \rangle}$$

$$y^* \triangleq \frac{y}{\frac{\mu}{\rho v_\tau}};$$

here, R^* is the von Kármán *number* (or rather: the von Kármán *distance*) and $y = R - r$; we see that $\frac{y}{R} = \frac{y^*}{R^*}$ and it is clear that τ_{w}, hence v_τ, is independent of r or y. It follows that[10]

$$\langle v \rangle = \frac{2\pi \int_0^R v\,(r)\,r dr}{\pi R^2} = -2\frac{\int_R^0 v\,(y) \cdot (R - y)\,dy}{R^2} = 2 \int_0^1 v\,(y) \left(1 - \frac{y}{R}\right) d\left(\frac{y}{R}\right)$$

$$\Downarrow$$

$$\frac{\langle v \rangle}{v_\tau} = 2 \int_0^1 v^* \left(\frac{y^*}{R^*}\right) \cdot \left(1 - \frac{y^*}{R^*}\right) d\left(\frac{y^*}{R^*}\right). \tag{6.23}$$

Power laws for v^* have been popular. One possible model is the one-seventh power law:

$$v^* = k \cdot (y^*)^{1/7} = k \cdot (R^*)^{1/7} \left(\frac{y^*}{R^*}\right)^{1/7}$$

which leads to

$$f_{\text{D}} = \frac{8}{\left(\frac{98k}{120 \cdot 2^{1/7}}\right)^{7/4}} \frac{1}{N_{\text{Re}}^{1/4}};$$

see Exercise 6.3. By curve fitting to data for a smooth pipe, Blasius[11] found (ca. 1913) $k = 8.56$, leading to

$$f_{\text{D}} = \frac{0.316}{N_{\text{Re}}^{1/4}} \Leftrightarrow f = \frac{0.079}{N_{\text{Re}}^{1/4}}, \tag{6.24}$$

which gives a good description for $N_{\text{Re}} \in (2.3 \times 10^3, 10^5)$.

For higher Reynolds numbers and a smooth pipe, Blasius' expression is not that good. An improved model for v^* could then be the "law of the wall" proposed by von Kármán[12] in 1930:

$$v^* = \frac{1}{\kappa} \ln\,(y^* + a^*) + C^* \tag{6.25}$$

where κ is the von Kármán *constant*, $a^* = \frac{a}{\frac{\mu}{\rho v_\tau}}$ is an offset parameter, while C^* is an additive constant, McKeon et al. (2005). In von Kármán's version, $a^* \equiv 0$, leading to

$$\sqrt{\frac{1}{f_{\text{D}}}} = -2 \cdot \log_{10} \left(\left(\frac{2 \cdot 2\sqrt{2}}{N_{\text{Re}}\sqrt{f_{\text{D}}}}\right)^{\frac{\ln(10)}{4\kappa\sqrt{2}}} \cdot 10^{\frac{\frac{3}{2} - \kappa C^*}{4\kappa\sqrt{2}}} \right), \tag{6.26}$$

---

[10]See Exercise 6.1.

[11]Paul Richard Heinrich Blasius, 1883–1970.

[12]Theodore von Kármán, 1881–1963 was a PhD student of Prandtl.

see Exercise 6.4. Assuming that C^* is independent of N_{Re} and f_{D}, Prandtl[13] found from curve fitting with the data of Nikuradse (see below) that

$$\frac{\ln(10)}{4\kappa\sqrt{2}} = 1 \Rightarrow \kappa = \frac{\ln(10)}{4\sqrt{2}} \approx 0.4070$$

and

$$4\sqrt{2} \cdot 10^{\frac{\frac{3}{2}-\kappa C^*}{4\kappa\sqrt{2}}} \approx 2.51$$

$$\Downarrow$$

$$C^* = \frac{3}{2\kappa} - 4\sqrt{2} \cdot \log_{10}\left(\frac{2.51}{4\sqrt{2}}\right) \approx 5.6814,$$

thus

$$\sqrt{\frac{1}{f_{\text{D}}}} = -2 \cdot \log_{10}\left(\frac{2.51}{N_{\text{Re}}} \cdot \frac{1}{\sqrt{f_{\text{D}}}}\right). \tag{6.27}$$

A modification of Prandtl's fitting has later been suggested as (Coelho & Pinho 2007)

$$\sqrt{\frac{1}{f_{\text{D}}}} = -2 \cdot \log_{10}\left(\frac{2.825}{N_{\text{Re}}} \cdot \frac{1}{\sqrt{f_{\text{D}}}}\right). \tag{6.28}$$

McKeon et al. (2005) suggest that for $N_{\text{Re}} \in (3.1 \times 10^5, 1.8 \times 10^7)$, a better expression is

$$\sqrt{\frac{1}{f_{\text{D}}}} = -1.93 \log_{10}\left(\frac{1}{N_{\text{Re}}} \frac{1}{\sqrt{f_{\text{D}}}}\right) - 0.537 = -2 \log_{10}\left(\frac{1.8557}{\left(N_{\text{Re}}\sqrt{f_{\text{D}}}\right)^{0.965}}\right). \tag{6.29}$$

6.4.1.7 Rough pipes and the Colebrook relation$^+$

Nikuradse[14] studied turbulent flow in rough pipes, described by the dimensionless ratio $\frac{\epsilon}{D}$ of the roughness height ϵ and the pipe diameter D, and fitted the data to the shape of the von Kármán relation, Eq. 6.26, leading to [15]

$$\frac{1}{\sqrt{f_{\text{D}}}} = 2 \cdot \log_{10}\left(\frac{3.71}{\epsilon/D}\right) = -2 \cdot \log_{10}\left(\frac{\epsilon/D}{3.71}\right). \tag{6.30}$$

Colebrook[16] considered how to merge Prandtl's fitting of von Kármán's model for smooth pipes with Nikuradse's model for rough pipes. The general problem is how to merge a model of type $k\log_{10} f_1(x)$ with a model of type $k\log_{10} f_2(x)$ into a global model $F(x)$, with $f_1(x) \gg f_2(x)$ for small values of x, and $f_1(x) \ll f_2(x)$ for large values of x, and with a smooth transition between the two functions. The relevance is that for small Reynolds numbers, $\frac{2.51}{N_{\text{Re}}\sqrt{f_{\text{D}}}} \gg \frac{\epsilon/D}{3.71}$, while for large

---

[13]Ludwig Prandtl, 1875 – 1953.

[14]Johann Nikuradse (1894–1979) was a PhD student of Ludwig Prandtl in 1920.

[15]Originally: $f_{\text{D}} = \frac{1}{\left(1.74 + 2\log_{10}\left(\frac{R}{\epsilon}\right)\right)^2}$, but this expression can be rewritten as $\frac{1}{\sqrt{f_{\text{D}}}} = 1.74 + 2\log_{10}\left(\frac{R}{\epsilon}\right) = 2\log_{10}\left(\sqrt{10^{1.74}}\right) + 2\log\left(\frac{R}{\epsilon}\right)$ or $\frac{1}{\sqrt{f_{\text{D}}}} = 2\log\left(\frac{\sqrt{10^{1.74}}}{2}\frac{D}{\epsilon}\right) = 2 \cdot \log_{10}\left(\frac{3.7066}{\epsilon/D}\right)$.

[16]C.F. Colebrook was at Imperial College, London.

Reynolds numbers, $\frac{2.51}{N_{\text{Re}}\sqrt{f_{\text{D}}}} \ll \frac{\epsilon/D}{3.71}$. Colebrook's observation was that with functions of type $f_1(x)$ and $f_2(x)$ as described above, a reasonable approximation could be

$$F(x) \triangleq k\log_{10}(f_1(x) + f_2(x)) \approx \begin{cases} k\log_{10}f_1(x), & x \text{ is small} \\ k\log_{10}f_2(x), & x \text{ is large.} \end{cases}$$

To this end, Colebrook proposed the following merging of the von Kármán–Prandtl model with Nikuradse's model:

$$\frac{1}{\sqrt{f_{\text{D}}}} = -2 \cdot \log_{10}\left(\frac{2.51}{N_{\text{Re}}} \cdot \frac{1}{\sqrt{f_{\text{D}}}} + \frac{\epsilon/D}{3.71}\right), \qquad (6.31)$$

which can be trivially modified, e.g., by replacing factor 2.51 with 2.825 (Coelho & Pinho 2007) or by using the expression of McKeon et al. (2005). Colebrook's relation is in general taken to be valid for $2.3 \times 10^3 < N_{\text{Re}} < 10^8$.

As an extension of the above idea, we observe that

$$k\log_{10}f(x) = \frac{k}{p}p\log_{10}f(x) = \frac{k}{p}\log_{10}f(x)^p.$$

It follows that we could more generally write

$$F(x) = \frac{k}{p}\log_{10}(f_1(x)^p + f_2(x)^p)$$

where $p > 0$, and where a large value for p $(p > 1)$ gives a more abrupt transition between $f_1(x)$ and $f_2(x)$. Thus, we could generalize Colebrook's model to

$$\frac{1}{\sqrt{f_{\text{D}}}} = -\frac{2}{p} \cdot \log_{10}\left(\left(\frac{2.51}{N_{\text{Re}}} \cdot \frac{1}{\sqrt{f_{\text{D}}}}\right)^p + \left(\frac{\epsilon/D}{3.71}\right)^p\right) \qquad (6.32)$$

with $p > 0$, typically $p \geq 1$; Colebrook's model has $p = 1$. The experimental results of McKeon et al. (2005) from the Princeton Superpipe seem to indicate that with $p = 1$, the estimate of f_{D} is slightly too large in the transition from smooth pipe to rough pipe dominance, thus it may be better to use $p > 1$.

6.4.1.8   Solution of Colebrook's relation by iteration[+]

As seen, Colebrook's relation is implicit in the unknown f_{D}, and it is not possible to find an explicit solution. To find a solution, iteration is thus needed. Iterative solutions need a first/seed value. Natural seed values could be based on explicit expressions, e.g., Blasius' smooth pipe expression ($\frac{0.316}{N_{\text{Re}}^{1/4}} = -2 \cdot \log_{10}\left(10^{-0.1508 \cdot N_{\text{Re}}^{-1/4}}\right)$), Nikuradse's rough pipe expression, or a combination of these:

$$\frac{1}{\sqrt{f_{\text{D}}^{(0)}}} = \begin{cases} 1/\sqrt{\frac{0.316}{N_{\text{Re}}^{1/4}}}, & \text{Blasius} \\ -2 \cdot \log_{10}\left(\frac{\epsilon/D}{3.71}\right), & \text{Nikuradse} \\ -\frac{2}{p} \cdot \log_{10}\left(10^{-\frac{0.316 \cdot p}{2} \cdot N_{\text{Re}}^{-1/4}} + \left(\frac{\epsilon/D}{3.71}\right)^p\right), & \text{Blasius-Nikuradse} \end{cases} \qquad (6.33)$$

and then compute refined approximations by *successive substitution*:

$$\frac{1}{\sqrt{f_{\mathrm{D}}^{(i+1)}}} = -\frac{2}{p} \cdot \log_{10}\left(\left(\frac{2.51}{N_{\mathrm{Re}}}\frac{1}{\sqrt{f_{\mathrm{D}}^{(i)}}}\right)^p + \left(\frac{\epsilon/D}{3.71}\right)^p\right). \qquad (6.34)$$

Using, e.g., the "Nikuradse" seed, successive substitution converges to an accurate solution in some 7 steps (Brkić 2011*b*).

Newton iteration is superior to successive substitution. To find a Newton iteration scheme, we introduce the "transmission" T:

$$T \triangleq \frac{1}{\sqrt{f_{\mathrm{D}}}}$$

and function $f(T)$ defined as

$$f(T) = T + \frac{2}{p} \cdot \log_{10}\left((aT)^p + b^p\right),$$

where we seek T such that $f(T) = 0$. The idea of Newton iteration is essentially to set the Taylor series expansion of $f(T)$ evaluated at iteration T_i, truncated after the linear term, equal to zero, and solve the linear equations to find T_{i+1}:

$$f(T_{i+1}) \approx f(T_i) + \left.\frac{\partial f}{\partial T}\right|_i (T_{i+1} - T_i) = 0$$

$$\Downarrow$$

$$T_{i+1} = T_i - \frac{f(T_i)}{\left.\frac{\partial f}{\partial T}\right|_i}.$$

Here,

$$\frac{\partial f}{\partial T} = 1 + \frac{2a}{\ln 10} \cdot \frac{(aT)^{p-1}}{(aT)^p + b^p}.$$

It follows that the Newton scheme for our generalized Colebrook relation is

$$\frac{1}{\sqrt{f_{\mathrm{D}}^{(i+1)}}} = \frac{1}{\sqrt{f_{\mathrm{D}}^{(i)}}} - \frac{\frac{1}{\sqrt{f_{\mathrm{D}}^{(i)}}} + \frac{2}{p} \cdot \log_{10}\left(\left(\frac{2.51}{N_{\mathrm{Re}}}\frac{1}{\sqrt{f_{\mathrm{D}}^{(i)}}}\right)^p + \left(\frac{\epsilon/D}{3.71}\right)^p\right)}{1 + \frac{2 \cdot \frac{2.51}{N_{\mathrm{Re}}}}{\ln 10} \cdot \frac{\left(\frac{2.51}{N_{\mathrm{Re}}}\frac{1}{\sqrt{f_{\mathrm{D}}^{(i)}}}\right)^{p-1}}{\left(\frac{2.51}{N_{\mathrm{Re}}}\frac{1}{\sqrt{f_{\mathrm{D}}^{(i)}}}\right)^p + \left(\frac{\epsilon/D}{3.71}\right)^p}},$$

with the obvious modifications if a or b are changed.

The Moody diagram in Fig. 6.6 is constructed from Eqs. 6.22 and 6.31, where we convert to Fanning's friction factor by using the relation $f_{\mathrm{D}} = 4f$.

6.4.1.9 Approximations to Colebrook's relation[+]

Approximations to the Colebrook relation are typically based on some direct explicit expressions, or by using the Lambert W function to solve the implicit expression — see Section 6.4.1.10 for a discussion on the Lambert W function.

In the sequel, the focus is on simple and efficient approximations of Colebrook's relation. Sections 6.4.1.8 gives an overview of iteration methods for Colebrook's relation. First, assume that the Blasius seed is used, Eq. 6.33:

$$\frac{1}{\sqrt{f_D^{(0)}}} = \frac{1}{\sqrt{\frac{0.316}{N_{Re}^{1/4}}}} = 1.7789 \cdot N_{Re}^{1/8}.$$

With one iteration of successive substitution, Eq. 6.34, this gives

$$\frac{1}{\sqrt{f_D^{(1)}}} = -\frac{2}{p} \cdot \log_{10}\left(\left(\frac{2.51}{N_{Re}}1.7789 \cdot N_{Re}^{1/8}\right)^p + \left(\frac{\epsilon/D}{3.71}\right)^p\right)$$

$$\Downarrow$$

$$\frac{1}{\sqrt{f_D}} \approx \frac{1}{\sqrt{f_D^{(1)}}} = -\frac{2}{p} \cdot \log_{10}\left(\left(\frac{4.4651}{N_{Re}^{0.875}}\right)^p + \left(\frac{\epsilon/D}{3.71}\right)^p\right), \qquad (6.35)$$

where normally $p = 1$. An alternative approach could be to use the Blasius relation as the initial guess in an iterator on Prandtl's smooth pipe relation to get

$$\frac{1}{\sqrt{f_D^{(1)}}} = -2 \cdot \log_{10}\left(\frac{4.4651}{N_{Re}^{0.875}}\right) = -2 \cdot \log_{10}\left(\left(\frac{5.5292}{N_{Re}}\right)^{0.875}\right).$$

Merging this expression with the von Karman expression similar as to Colebrook's approach, we get

$$\frac{1}{\sqrt{f_D}} \approx -\frac{2}{p} \cdot \log\left(\left(\frac{5.5292}{N_{Re}}\right)^{0.875 \cdot p} + \left(\frac{\epsilon/D}{3.71}\right)^p\right). \qquad (6.36)$$

If we choose the log argument to be linear in $1/N_{Re}$, we have $p = \frac{1}{0.875} \approx 1.1429$ and $\frac{2}{p} = 1.75$. Alternatively, we could set $p = 1$ with $5.5292^{0.875} \approx 4.4651$. If coefficient 2.51 in the original Colebrook relation is replaced by value 2.825 as indicated in Eq. 6.28, we find $5.5292 \rightarrow 6.329$ with $6.329^{0.875} \approx 5.0254$.

Table 6.2 gives a summary of some approximations.

All approximations in Table 6.2 seem to be based on some successive substitution approach, with 1–2 iterations. It is not really meaningful to compare Haaland's gas expression in Table 6.2 with Colebrook's original relation with $p = 1$. See Brkić (2011b) for a comprehensive, updated review of approximations to Colebrook's formula.[17] Newton iterations would be more accurate, but slightly more complex.

If it is desirable to use Fanning's friction factor instead of Darcy's friction factor, the conversion is simple: $f = f_D/4$.

6.4.1.10   Colebrook's relation and the Lambert W function[+]

We consider Colebrook's relation with Darcy friction as in Eq. 6.31.

---

[17]See also `https://en.wikipedia.org/wiki/Darcy_friction_factor_formulae`.

Table 6.2: Simple, explicit approximations of Colebrook's relation, with maximal deviation (Max dev) from Colebrook's relation over the region $N_{\mathrm{Re}} \in [10^4, 10^8]$ and $\frac{\epsilon}{D} \in [10^{-1}, 10^{-6}]$. See Brkić (2011b).

Approximation	Max dev	Method
$\frac{1}{\sqrt{f_{\mathrm{D}}}} = -2 \cdot \log_{10}\left(\frac{15}{N_{\mathrm{Re}}} + \frac{\epsilon/D}{3.715}\right)$	8.2%	Eck, 1973
$\frac{1}{\sqrt{f_{\mathrm{D}}}} = -2 \cdot \log\left(\frac{5.7622}{N_{\mathrm{Re}}^{0.9}} + \frac{\epsilon/D}{3.71}\right)$	2.18%	Churchill, 1973. Observe the similarity to Eq. 6.36 with $p = 1$.
$\frac{1}{\sqrt{f_{\mathrm{D}}}} = -2 \cdot \log\left(\frac{5.74}{N_{\mathrm{Re}}^{0.9}} + \frac{\epsilon/D}{3.7}\right)$	2.04%	Swamee and Jain, 1976; tuning of Churchill, 1973.
$\frac{1}{\sqrt{f_{\mathrm{D}}}} = -2 \cdot \log\left(\frac{5.72}{N_{\mathrm{Re}}^{0.9}} + \frac{\epsilon/D}{3.715}\right)$	2.05%	Jain, 1976; tuning of Churchill, 1973.
$\frac{1}{\sqrt{f_{\mathrm{D}}}} \approx -1.8 \cdot \log\left(\frac{6.9}{N_{\mathrm{Re}}} + \left(\frac{\epsilon/D}{3.7}\right)^{1.11}\right)$	1.4%	Haaland, 1983, for liquid; similar to Eq. 6.36 with $0.875 \cdot p = 1$.
$\frac{1}{\sqrt{f_{\mathrm{D}}}} \approx -\frac{1.8}{3} \cdot \log\left(\left(\frac{6.9}{N_{\mathrm{Re}}}\right)^3 + \left(\frac{\epsilon/D}{3.7}\right)^{1.11 \cdot 3}\right)$	—	Haaland, 1983, for gas; similar to Eq. 6.36 with $0.875 \cdot p = 3$.
$\frac{1}{\sqrt{f_{\mathrm{D}}^{(0)}}} = -2.01 \cdot \log_{10}\left(\frac{5.8506}{N_{\mathrm{Re}}^{0.8981}} + \frac{(\epsilon/D)^{1.1098}}{2.8257}\right)$	0.35%	Chen, 1979: seed $\frac{1}{\sqrt{f_{\mathrm{D}}^{(0)}}}$; $f_{\mathrm{D}} \approx f_{\mathrm{D}}^{(1)}$ based on Eq. 6.34 with "3.71" replaced by "3.71065"
$\frac{1}{\sqrt{f_{\mathrm{D}}^{(0)}}} = -2 \cdot \log_{10}\left(\frac{13}{N_{\mathrm{Re}}} + \frac{\epsilon/D}{3.7}\right)$	1%	Zigrang and Sylvester, 1982: seed $\frac{1}{\sqrt{f_{\mathrm{D}}^{(0)}}}$ similar to Eck, 1973; $f_{\mathrm{D}} \approx f_{\mathrm{D}}^{(1)}$ based on Eq. 6.34 with "3.71" replaced by "3.7"
$\frac{1}{\sqrt{f_{\mathrm{D}}^{(0)}}} = -2 \cdot \log_{10}\left(\frac{13}{N_{\mathrm{Re}}} + \frac{\epsilon/D}{3.7}\right)$	0.13%	Zigrang and Sylvester, 1982: seed $\frac{1}{\sqrt{f_{\mathrm{D}}^{(0)}}}$ similar to Eck, 1973; $f_{\mathrm{D}} \approx f_{\mathrm{D}}^{(2)}$ with $f_{\mathrm{D}}^{(1)}, f_{\mathrm{D}}^{(2)}$ based on Eq. 6.34 with "3.71" replaced by "3.7"

Theorem 6.1. *Colebrook's relation can alternatively be expressed as*

$$W \cdot \exp\left(W\right) = x$$

where

$$x = \frac{N_{\mathrm{Re}}}{2.51} \frac{\ln 10}{2} \exp\left(\frac{N_{\mathrm{Re}}}{2.51} \frac{\ln 10}{2} \frac{\epsilon/D}{3.71}\right)$$

$$W = \frac{N_{\mathrm{Re}}}{2.51} \frac{\ln 10}{2} z$$

and

$$z = \frac{2.51}{N_{\mathrm{Re}}} \frac{1}{\sqrt{f_{\mathrm{D}}}} + \frac{\epsilon/D}{3.71}.$$

▲

Proof. For Colebrook's relation in Eq. 6.31, introduce z,

$$z = \frac{2.51}{N_{\mathrm{Re}}} \frac{1}{\sqrt{f_{\mathrm{D}}}} + \frac{\epsilon/D}{3.71}$$

$$\Downarrow$$

$$\frac{1}{\sqrt{f_{\mathrm{D}}}} = \frac{N_{\mathrm{Re}}}{2.51}\left(z - \frac{\epsilon/D}{3.71}\right),$$

which when inserted into Colebrook's relation gives

$$\frac{N_{\mathrm{Re}}}{2.51}\left(z - \frac{\epsilon/D}{3.71}\right) = -2 \cdot \log_{10} z$$

$$\Downarrow$$

$$\frac{N_{\mathrm{Re}}}{2.51} \frac{\ln 10}{2}\left(z - \frac{\epsilon/D}{3.71}\right) = -\ln z = \ln\left(\frac{1}{z}\right)$$

or

$$\frac{1}{z} = \exp\left(\frac{N_{\mathrm{Re}}}{2.51} \frac{\ln 10}{2} z\right) \exp\left(-\frac{N_{\mathrm{Re}}}{2.51} \frac{\ln 10}{2} \frac{\epsilon/D}{3.71}\right)$$

which can be rewritten into

$$\exp\left(\frac{N_{\mathrm{Re}}}{2.51} \frac{\ln 10}{2} \frac{\epsilon/D}{3.71}\right) = z \cdot \exp\left(\frac{N_{\mathrm{Re}}}{2.51} \frac{\ln 10}{2} z\right)$$

$$\Downarrow$$

$$\frac{N_{\mathrm{Re}}}{2.51} \frac{\ln 10}{2} \exp\left(\frac{N_{\mathrm{Re}}}{2.51} \frac{\ln 10}{2} \frac{\epsilon/D}{3.71}\right) = \frac{N_{\mathrm{Re}}}{2.51} \frac{\ln 10}{2} z \cdot \exp\left(\frac{N_{\mathrm{Re}}}{2.51} \frac{\ln 10}{2} z\right).$$

Here, let

$$W = \frac{N_{\mathrm{Re}}}{2.51} \frac{\ln 10}{2} z$$

$$x = \frac{N_{\mathrm{Re}}}{2.51} \frac{\ln 10}{2} \exp\left(\frac{N_{\mathrm{Re}}}{2.51} \frac{\ln 10}{2} \frac{\epsilon/D}{3.71}\right)$$

and Colebrook's relation can be written as

$$W \cdot \exp\left(W\right) = x \tag{6.37}$$

with solution $W\left(x\right)$.   □
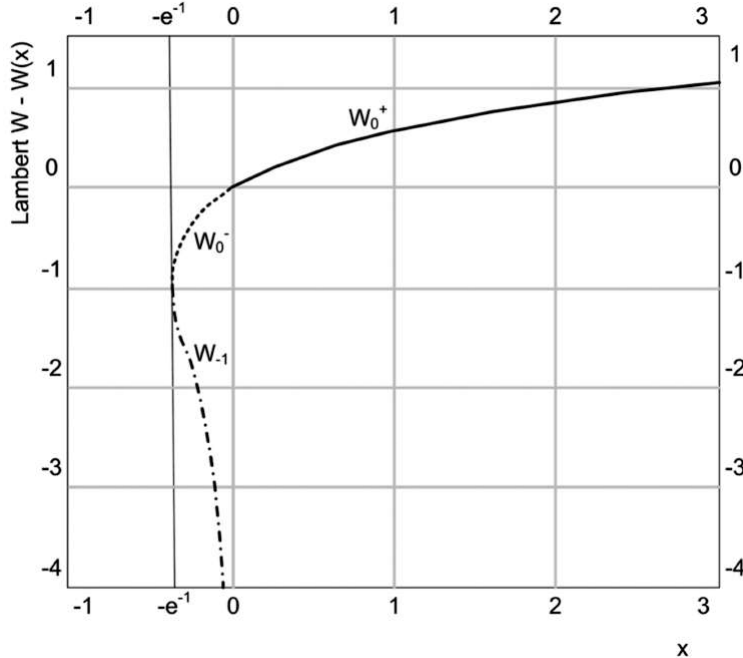
Figure 6.8: x, W relation between x and the Lambert "function" W showing two branches (functions) $W_{-1}(x)$ and $W_0(x)$. The so-called *principal branch* W_0 can be split into W_0^- valid for $x \in \left[-\frac{1}{\exp(1)}, 0\right)$ and W_0^+ valid for $x \geq 0$. From Brkić (2011*a*).

Remark 6.1. The solution $W(x)$ to $W \cdot \exp(W) = x$ is given by Lambert's W function. Solving Colebrook's implicit relation has thus been rephrased into solving the implicit relation in Eq. 6.37. This implicit relation is a standard form in mathematics, which can be solved using the so-called *Lambert W function*. There is no magic in the Lambert W function, though — iterations are necessary to find the solution. The advantage with using Lambert's W function, is that it has been thoroughly studied in (numerical) mathematics. ▲

In general, W and x can be complex numbers, but here, x is a real number, and W is a real number. The pair (x, W) constitute a *relation*,[18] see Fig. 6.8.

$W(x)$ is a relation since $W(x)$ is two-valued in the region $x \in \left[-\frac{1}{\exp(1)}, 0\right)$. The principal branch $W_0(x)$ (Fig. 6.8) is a strictly increasing function.

From Theorem 6.1, we see that both x and W must be positive numbers, hence

---

[18]Relations are generalizations of functions to allow for multi-valued mappings.

we are interested in the function $W_0^+(x)$, where $W_0^+(0) = 0$. Recursively, we have

$$W \cdot \exp(W) = x$$
$$\Downarrow$$
$$W = x \cdot \exp(-W)$$
$$\Downarrow$$
$$W = x \cdot \exp(-x \cdot \exp(-W))$$
$$\Downarrow$$
$$W = x \cdot \exp(-x \cdot \exp(-x \cdot \exp(-x \cdot (\cdots))));$$

it can be shown that when $x \to 0$, this recursion can be truncated to give an approximation of $W(x)$ (Barry et al. 1995). If we instead are interested in large values of x $(x \to \infty)$, we can instead rewrite the expression as

$$W \cdot \exp(W) = x$$
$$\Downarrow$$
$$\exp(\ln W) \cdot \exp(W) = x$$
$$\Downarrow$$
$$\exp(\ln W + W) = x$$
$$\Downarrow$$
$$W = \ln x - \ln W = \ln \frac{x}{W}$$
$$\Downarrow$$
$$W = \ln \frac{x}{\ln \frac{x}{\ln \frac{x}{\cdots}}}.$$

This recursion can be truncated to given an approximation of $W(x)$ for large x.

In Barry et al. (2000), a relatively simple and accurate approximation W_0^{+*2} for W_0^+ is developed:

$$W_0^{+*2}(x) = (1 + \varepsilon) \ln \left(\frac{6x}{5 \ln \left[\frac{12}{5} \frac{x}{\ln\left(1 + \frac{12}{5}x\right)} \right]} \right) - \varepsilon \ln \left(\frac{2x}{\ln(1+x)} \right) \qquad (6.38)$$

where $\varepsilon \approx 0.4586887$, with maximal error 0.196%. A procedure for finding more accurate approximations is also given.

The procedure for solving Colebrook's relation using the Lambert W function is thus as follows, Theorem 6.1:

1. With given ratio ϵ/D and N_{Re}, compute x from

$$x = \frac{N_{\mathrm{Re}}}{2.51} \frac{\ln 10}{2} \exp \left(\frac{N_{\mathrm{Re}}}{2.51} \frac{\ln 10}{2} \frac{\epsilon/D}{3.71} \right).$$

2. Next, with x known, compute $W(x)$, e.g., via the approximation $W_0^{+*2}(x)$, Eq. 6.38.

3. Next, find z from

$$W = \frac{N_{\mathrm{Re}}}{2.51} \frac{\ln 10}{2} z \Rightarrow z = \frac{2.51}{N_{\mathrm{Re}}} \frac{2}{\ln 10} W \approx \frac{2.51}{N_{\mathrm{Re}}} \frac{2}{\ln 10} W_0^{+*2}.$$

4. Finally, find $\frac{1}{\sqrt{f_{\mathrm{D}}}}$ from

$$z = \frac{2.51}{N_{\mathrm{Re}}} \frac{1}{\sqrt{f_{\mathrm{D}}}} + \frac{\epsilon/D}{3.71} \Rightarrow \frac{1}{\sqrt{f_{\mathrm{D}}}} = \frac{N_{\mathrm{Re}}}{2.51} \left(z - \frac{\epsilon/D}{3.71} \right).$$

See also Brkić (2011*a*).

6.4.1.11 Global friction factor models^{+}

It may be of interest with a friction factor model that spans both the laminar and the turbulent regions, i.e., global models. One such model is due to Churchill, 1977 (Brkić 2011*b*), and is valid for $0 < N_{\mathrm{Re}} < 10^8$:

$$f_{\mathrm{D}} = 8 \left(\left(\frac{8}{N_{\mathrm{Re}}} \right)^{12} + \frac{1}{(C_1 + C_2)^{1.5}} \right)^{\frac{1}{12}}$$

where

$$C_1 = \left(2.457 \ln \frac{1}{\left(\frac{7}{N_{\mathrm{Re}}} \right)^{0.9} + 0.27 \frac{\epsilon}{D}} \right)^{16}$$

$$C_2 = \left(\frac{37530}{N_{\mathrm{Re}}} \right)^{16}.$$

Alternatively, one could use the idea of Colebrook and write

$$f_{\mathrm{D}} = \frac{64}{N_{\mathrm{Re}}} \Rightarrow \frac{1}{\sqrt{f_{\mathrm{D}}}} = \frac{N_{\mathrm{Re}}^{1/2}}{8} = -\frac{2}{p} \cdot \log_{10} 10^{-\frac{N_{\mathrm{Re}}^{1/2}}{16} \cdot p}$$

which can then be merged with the Colebrook relation into

$$\frac{1}{\sqrt{f_{\mathrm{D}}}} = -\frac{2}{p} \cdot \log_{10} \left(10^{-\frac{N_{\mathrm{Re}}^{1/2}}{16} \cdot p} + \left(\frac{2.51}{N_{\mathrm{Re}}} \cdot \frac{1}{\sqrt{f_{\mathrm{D}}}} \right)^p + \left(\frac{\epsilon/D}{3.71} \right)^p \right). \tag{6.39}$$

Yet another possibility is to use some interpolation expression between the laminar value at $N_{\mathrm{Re}} = 2100$ and the turbulent value at $N_{\mathrm{Re}} = 2300$, e.g., linear interpolation — or if the friction factor should be differentiable: a cubic polynomial fitting with the same slope as laminar friction at $N_{\mathrm{Re}} = 2100$ and turbulent friction at $N_{\mathrm{Re}} = 2300$. To achieve global differentiability, with $p(N_{\mathrm{Re}}) = aN_{\mathrm{Re}}^3 + bN_{\mathrm{Re}}^2 + cN_{\mathrm{Re}} + d$, thus

$$p(N_{\mathrm{Re}} = 2100) = f_{\mathrm{D}}^{\ell}(N_{\mathrm{Re}} = 2100)$$

$$p(N_{\mathrm{Re}} = 2300) = f_{\mathrm{D}}^{\mathrm{t}}(N_{\mathrm{Re}} = 2300)$$

$$\left. \frac{dp}{dN_{\mathrm{Re}}} \right|_{N_{\mathrm{Re}}=2100} = \left. \frac{df_{\mathrm{D}}^{\ell}}{dN_{\mathrm{Re}}} \right|_{N_{\mathrm{Re}}=2100}$$

$$\left. \frac{dp}{dN_{\mathrm{Re}}} \right|_{N_{\mathrm{Re}}=2300} = \left. \frac{\partial f_{\mathrm{D}}^{\mathrm{t}}}{\partial N_{\mathrm{Re}}} \right|_{\frac{\epsilon}{D}, N_{\mathrm{Re}}=2300},$$

which gives rise to 4 linear equations in the four unknowns (a, b, c, d).

In some cases where a "global" expression for f_D could be useful, the average velocity will oscillate around zero, i.e., change direction.[19] With $\langle v \rangle \to 0 \Rightarrow f_D \to \infty$, which is not really useful. Instead, it is better to consider the friction force directly:

$$F_f = K''' A_w f \Rightarrow \frac{F_f}{A_w} = \frac{1}{2} \rho \langle v \rangle^2 \cdot \frac{16}{N_{Re}} = 8 \cdot \frac{\rho \langle v \rangle^2}{\frac{\rho \langle v \rangle D}{\mu}} = 8 \cdot \frac{\mu \langle v \rangle}{D}$$

$$\Downarrow$$

$$F_f = 8 \cdot \frac{\mu \langle v \rangle}{D} A_w = 8 \cdot \frac{\mu \langle v \rangle}{D} \pi D L = 8\pi \cdot \mu \langle v \rangle L. \tag{6.40}$$

where it clear that friction force F_f is *directed opposite* to $\langle v \rangle$.

6.4.2   Pressure drop due to constrictions, etc.

We have seen that the pressure drop in a long, straight pipe is

$$\Delta p_f = \frac{1}{A} F_f = \tau_w \frac{A_w}{A}.$$

where we utilized that

$$\tau_w = f \cdot K''' = f_D \frac{1}{4} K'''.$$

With a cylindrical pipe, we have $\frac{A_w}{A} = \frac{\pi D L}{\pi \frac{D^2}{4}} = \frac{4L}{D}$, and it follows that

$$\Delta p_f = f_D \frac{L}{D} K'''.$$

Inspired by this, we could write the friction pressure drop as

$$\Delta p_f = \phi K''' \tag{6.41}$$

where dimensionless factor ϕ is $\phi = f_D \frac{L}{D}$ for a long, straight pipe. We will refer to ϕ as the generalized friction factor.[20]

What if we instead of a long, straight pipe have various contractions, enlargements, bends, etc.? It turns out that we for those cases also can write the pressure drop as in Eq. 6.41. Tables 6.3–6.4 illustrate some cases.

6.4.3   Liquid friction in open channel

In open channels, it is common to introduce the co-called (steady) friction slope S_{fs}, which can be expressed as

$$S_{fs} \triangleq \frac{F'_{fs}}{\rho g A_s}.$$

Table 6.3: Generalized friction factor ϕ for various fittings, valves, etc. For Reynolds number N_{Re} and Darcy friction coefficient f_{D}, this refers to the entrance velocity $\langle v \rangle_1$ and diameter D_1.   See also Table 6.4. Taken from `https://neutrium.net/fluid_flow/pressure-loss-from-fittings-expansion-and-reduction-in-pipe-size/`.
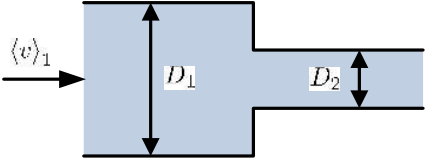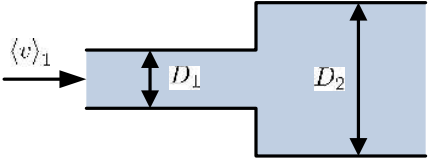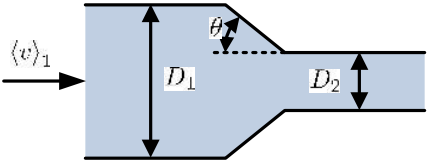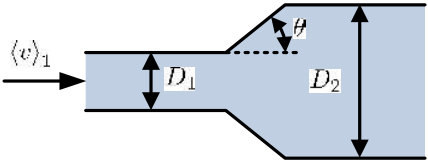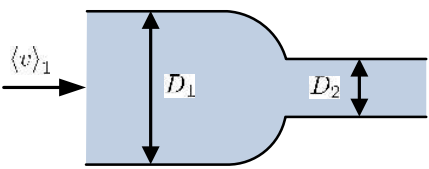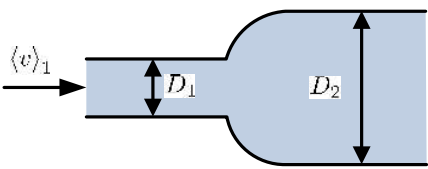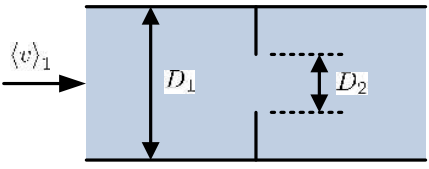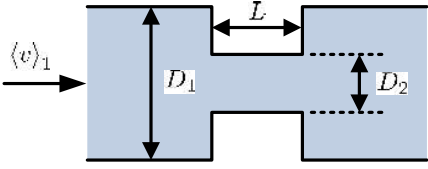
Square reduction	*Square expansion*

$N_{\mathrm{Re}} < 2500$:

$$\phi_{\mathrm{sr}} = \left(1.2 + \frac{160}{N_{\mathrm{Re}}}\right)\left[\left(\frac{D_1}{D_2}\right)^4 - 1\right]$$

$N_{\mathrm{Re}} \geq 2500$:

$$\phi_{\mathrm{sr}} = (0.6 + 0.48 f_{\mathrm{D}})\left(\frac{D_1}{D_2}\right)^2\left[\left(\frac{D_1}{D_2}\right)^2 - 1\right]$$

$N_{\mathrm{Re}} < 4000$:

$$\phi_{\mathrm{se}} = 2\left[1 - \left(\frac{D_1}{D_2}\right)^4\right]$$

$N_{\mathrm{Re}} \geq 4000$:

$$\phi_{\mathrm{se}} = (1 + 0.8 f_{\mathrm{D}})\left[1 - \left(\frac{D_1}{D_2}\right)^2\right]^2$$

Tapered reduction	*Tapered expansion*

$\theta \in [0, 22.5\,°]$:
$\phi_{\mathrm{tr}} = 1.6 \cdot \sin\left(\frac{\theta}{4}\right) \cdot \phi_{\mathrm{sr}}$
$\theta \in (22.5\,°, 90\,°)$:
$\phi_{\mathrm{tr}} = \sqrt{\sin\left(\frac{\theta}{4}\right)} \cdot \phi_{\mathrm{sr}}$

$\theta \in [0, 22.5\,°]$:
$\phi_{\mathrm{te}} = 2.6 \cdot \sin\left(\frac{\theta}{4}\right) \cdot \phi_{\mathrm{se}}$
$\theta \in (22.5\,°, 90\,°)$:
$\phi_{\mathrm{te}} = \phi_{\mathrm{se}}$

Table 6.4:   Generalized friction factor ϕ for various fittings, valves, etc. For Reynolds number N_{Re} and Darcy friction coefficient f_{D}, this refers to the entrance velocity $\langle v \rangle_1$ and diameter D_1.   See also Table 6.3. Taken from `https://neutrium.net/fluid_flow/pressure-loss-from-fittings -expansion-and-reduction-in-pipe-size/`.

Rounded reduction	*Rounded expansion*

$$\phi_{\mathrm{rr}} = \left(0.1 + \frac{50}{N_{\mathrm{Re}}}\right)\left[\left(\frac{D_1}{D_2}\right)^4 - 1\right] \qquad \phi_{\mathrm{re}} = \phi_{\mathrm{se}}$$

Sharp orifice	*Thick Orifice*

$N_{\mathrm{Re}} < 2500$:

$$\phi_{\mathrm{so}} = \left[2.72 + \left(\frac{D_2}{D_1}\right)^2\left(\frac{120}{N_{\mathrm{Re}}} - 1\right)\right] \cdot \phi_{\mathrm{so}}^0$$

$N_{\mathrm{Re}} \geq 2500$:

$$\phi_{\mathrm{so}} = \left[2.72 + \left(\frac{D_2}{D_1}\right)^2 \cdot \frac{4000}{N_{\mathrm{Re}}}\right] \cdot \phi_{\mathrm{so}}^0$$

where $\phi_{\mathrm{so}}^0 = \left[1 - \left(\frac{D_2}{D_1}\right)^2\right]\left[\left(\frac{D_1}{D_2}\right)^4 - 1\right]$.

$\frac{L}{D_2} \leq 5$:

$$\phi_{\mathrm{to}} = \left(0.584 + \frac{0.0936}{\left(\frac{L}{D_2}\right)^{1.5} + 0.225}\right) \cdot \phi_{\mathrm{so}}$$

$\frac{L}{D_2} > 5$:

*Square reduction* followed by

square expansion
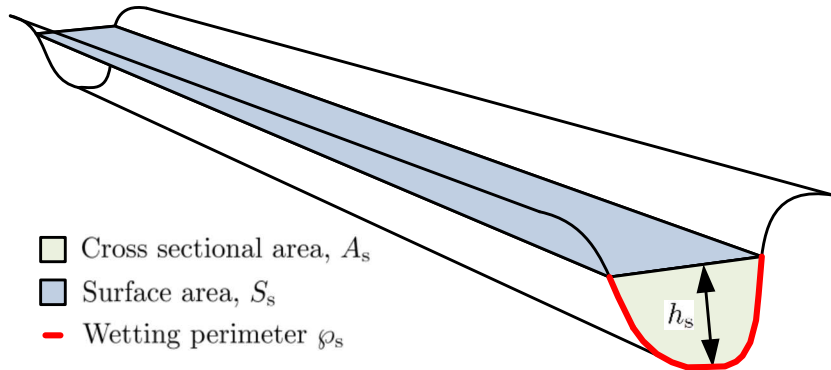
Figure 6.9: Nomenclature for open channel flow.

Here, F'_{fs} is the (steady) friction force per unit length of the channel, ρ is the density of the liquid, g is gravity, and A_{s} is the cross sectional area of the liquid in the channel; Fig. 6.9.

For open channel flow of Newtonian liquids, it is common to describe the friction slope S_{fs} using the Gauckler–Manning–Strickler formula

$$v_{\text{s}} = \frac{\dot{V}_{\text{s}}}{A_{\text{s}}} = \frac{1}{k_{\text{M}}} R_{\text{s}}^{2/3} S_{\text{fs}}^{1/2},$$

where k_{M} is *Manning's friction coefficient* (sometimes denoted n) while R_{s} is the hydraulic radius defined as

$$R_{\text{s}} = \frac{A_{\text{s}}}{\wp_{\text{s}}}$$

— the ratio of the cross sectional area A_{s} and the wetting perimeter $\wp_{\text{s}}$. It follows that we can express S_{fs} as

$$\frac{\dot{V}_{\text{s}}}{A_{\text{s}}} = \frac{1}{k_{\text{M}}} R_{\text{s}}^{2/3} S_{\text{fs}}^{1/2}$$
$$\Downarrow$$
$$S_{\text{fs}} = k_{\text{M}}^2 \frac{\left(\frac{\dot{V}_{\text{s}}}{A_{\text{s}}}\right)^2}{R_{\text{s}}^{4/3}} = k_{\text{M}}^2 \frac{\left(\frac{\dot{V}_{\text{s}}}{A_{\text{s}}}\right)^2 \wp_{\text{s}}^{4/3}}{A_{\text{s}}^{4/3}}.$$

It is of interest to compare this friction slope with the result obtained by using the Friction force in Eq. 6.17. If we simplify the expression for S_{fs} above somewhat using the approximation

$$\left(\frac{\wp_{\text{s}}}{A_{\text{s}}}\right)^{\frac{4}{3}} \approx \frac{\wp_{\text{s}}}{A_{\text{s}}},$$

---

[19]This is the case, e.g., in the surge tank of a high pressure hydro power plant.

[20]In `https://neutrium.net/fluid_flow/pressure-loss-from-fittings-expansion-and-reduction-in-pipe-size/`, this "generalized friction factor" is referred to as the K-value, while Lydersen (1979) refer to is as n.

Table 6.5: Examples of values for Manning's friction factor k_M.

Bed material	Manning factor k_{M}
Asphalt	0.016
Brick	0.015
Clay tile	0.014
Concrete - steel forms	0.011
Concrete (Cement) - finished	0.012
Concrete - wooden forms	0.015
Earth, smooth	0.018
Earth channel - clean	0.022
Earth channel - gravelly	0.025
Earth channel - weedy	0.030
Earth channel - stony, cobbles	0.035
Floodplains - pasture, farmland	0.035
Floodplains - light brush	0.050
Floodplains - heavy brush	0.075
Floodplains - trees	0.15
Natural streams - clean and straight	0.030
Natural streams - major rivers	0.035
Natural streams - sluggish with deep pools	0.040
Natural channels, very poor condition	0.060
Wood - planed	0.012
Wood - unplaned	0.013

we see that the friction slope becomes

$$S_{\mathrm{fs}} = k_{\mathrm{M}}^2 \frac{\left(\frac{\dot{V}_{\mathrm{s}}}{A_{\mathrm{s}}}\right)^2 \wp_{\mathrm{s}}}{A_{\mathrm{s}}} = k_{\mathrm{M}}^2 \frac{v_{\mathrm{s}}^2 \wp_{\mathrm{s}}}{A_{\mathrm{s}}}.$$

On the other hand, from Eq. 6.17, we have

$$F_{\mathrm{fs}} = K_{\mathrm{s}}''' A_{\mathrm{s}} f = \frac{1}{2} \rho v_{\mathrm{s}}^2 \wp_{\mathrm{s}} L f \Rightarrow F_{\mathrm{f}}' = \frac{1}{2} \rho v_{\mathrm{s}}^2 \wp_{\mathrm{s}} f,$$

thus the friction slope from this expression is

$$S_{\mathrm{fs}} = \frac{F_{\mathrm{fs}}'}{\rho g A_{\mathrm{s}}} = \frac{\frac{1}{2} \rho v_{\mathrm{s}}^2 \wp_{\mathrm{s}} f}{\rho g A_{\mathrm{s}}} = \frac{f}{2g} \frac{v_{\mathrm{s}}^2 \wp_{\mathrm{s}}}{A_{\mathrm{s}}}.$$

We see that Manning's friction factor k_{M} is approximately

$$k_{\mathrm{M}}^2 \approx \frac{f}{2g}.$$

Some typical values for Manning's friction factor are given in Table 6.5.[21]

When used for flow of water in rivers, *Manning*'s friction coefficient k_{M} typically varies from 0.03 in clean and straight river beds to 0.06 for poorly conditioned

---

[21]Taken from `www.engineeringtoolbox.com/mannings-roughness-d_799.html`

channel beds. A typical value for *Fanning*'s friction factor under turbulent flow in hydraulically *smooth pipes* is $f \in [0.002, 0.005]$, Bird et al. (2002), which would lead to $\sqrt{\frac{f}{2g}} \in [0.01, 0.016]$. For turbulent flow in less smooth pipes, the Fanning friction factor f can have a value of up to 0.01, which would lead to $\sqrt{\frac{f}{2g}} = 0.02$ Thus, values for Manning's friction coefficient appear to be compatible with Fanning's friction factor.

6.4.4   Power consumption in agitated liquid tanks

In Problem 2.2 p. 41, the task is to show that for agitation of a liquid tank,

$$\frac{\dot{W}}{\rho D_i^5 \dot{n}_i^3} = f\left(N_{\mathrm{Re}}\right)$$

where $\dot{W}$ is the power consumption used for agitating the liquid tank, ρ is the liquid density, D_i is the impeller diameter, and $\dot{n}_i$ is the number of revolutions per time unit of the impeller. f is a friction factor ("power number") and the Reynolds number for agitation is[22]

$$N_{\mathrm{Re}} = \frac{\rho \dot{n}_i D_i^2}{\mu}$$

where μ is the liquid viscocity.

The power consumption essentially is dissipated power by friction between the impeller blades and the liquid. Thus the shaft power $\dot{W}$ essentially is equal to the friction power $\dot{W}_f$ for the rotating liquid of the tank, hence

$$\dot{W}_f = -\rho D_i^5 \dot{n}_i^3 f. \tag{6.42}$$

Figure 6.10 shows the agitation friction factor ("power number") for some impeller geometries.

6.5   Compressible fluid. Elasticity of walls⋆

...under construction...

6.6   Turbo machines⋆

A turbo-machine is a machine which transfers energy between a continuous stream of a fluid and an element rotating about a fixed axis, Turton (1995). Examples of turbo-machines are pumps, fans, compressors, and turbines. In pumps (liquid) and fans and compressors (gas), mechanical power is added through the rotating axis and leads to an increase in the fluid pressure over the equipment, while turbines

---

[22]Normally, Reynolds' number is expressed as $\frac{\rho v D}{\mu}$. Observe that $\dot{n}_i = \frac{\omega_i}{2\pi}$ where ω_i is angular velocity, thus the velocity at the impeller tip is $v = \omega_i \frac{D_i}{2}$. Thus, $N_{\mathrm{Re}} = \frac{\rho \dot{n}_i D_i^2}{\mu} = \frac{\rho \omega_i D_i^2}{2\pi\mu} = \frac{\rho v D_i}{\mu} \frac{1}{4\pi}$.

No.	Type of impeller		$\dfrac{D_t}{D_i}$	$\dfrac{z_e}{z_i}$	$\dfrac{z_i}{D_i}$	Baffles Number	B/D_i
1	Turbine with 6 vanes		3	2.7 −3.9	0.75 −1.3	4	0.10
2	Plate with 16 vanes		2.5	2.5	0.75	4	0.25
3	Paddle with 2 blades		3	2.7 −3.9	0.75 −1.3	4	0.10
4	Propeller with 3 blades, pitch $h = D_i$		3	2.7 −3.9	0.75 −1.3	4	0.10

$$N_{Re} = \frac{\rho \dot{n}_i D_i^2}{\mu}$$
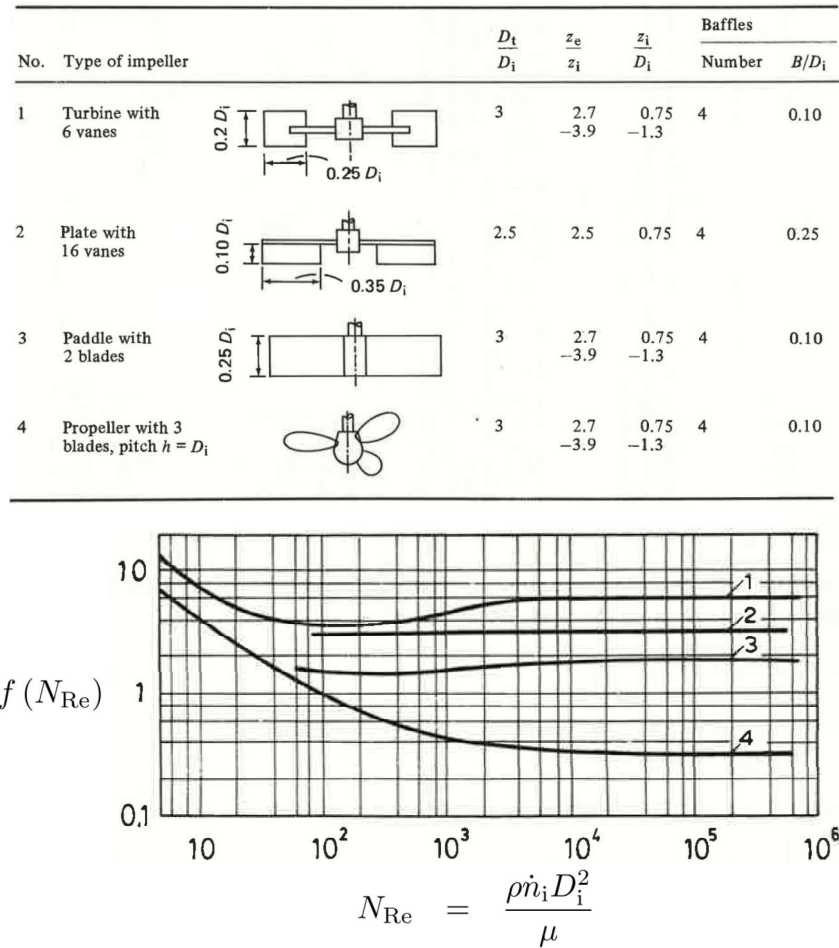
Figure 6.10: Agitation friction factor f ("power number") as a function of Reynolds number N_{Re} for some impeller geometries (Lydersen 1979). In the upper figure, D_i is the impeller diameter, D_t is the tank diameter, h is the propeller pitch (No. 4), z_i is the height of impeller above bottom, z_e is the liquid level in the tank, and B is the width of baffles. In the curves of the lower figure, the curve numbers (1–4) refer to the configuration row in the upper figure.
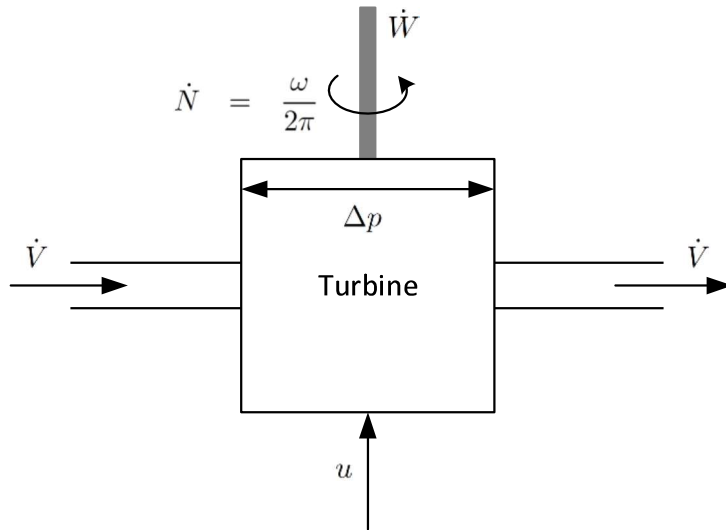
Figure 6.11: Key quantities in a turbine.

convert a pressure drop in the fluid across the machine into mechanical power on the rotating axis.

...under construction...

- Start with dimensionless model/dimensional analysis

- Transport equipment: fan (gas, low pressure), compressor (gas, high pressure), pump (liquid) ... role of energy balance?

- Energy extraction: turbine (gas, liquid)

Pump model: providing power to pump the fluid, fluid flows through the pump at volumetric flow rate $\dot{V}_p$ while increasing the pressure over the pump by Δp_p. A typical model for the pressure increase is

$$\Delta p_p = f(u)\left(\Delta p_p^\varsigma - \delta p_{\dot{V}_p}\left(\frac{\dot{V}_p}{\dot{V}_p^\varsigma}\right)^2\right)$$

where u is an input signal that governs the provided power.

6.6.1 Turbines

In hydro turbines, water flows at volumetric flow rate $\dot{V}$ (volume/time) through the machine, and part of the pressure drop Δp in the water is converted to mechanical power $\dot{W}$ on the axis rotating at speed $\dot{N}$ (revolutions/time), while an additional pressure drop is due to friction/losses. An actuator signal u may change the opening in the fluid passage and change the pressure drop and mechanical power produced.

Figure 6.11 indicates the key quantities for a turbine.

In practical operation, some of the variables are given by the environment to the turbine — these variables are specified as *boundary conditions* for the turbine, while the turbine itself determines the remaining variables.

The boundary conditions for the turbine are the following:

- the volumetric flow rate $\dot{V}$ is a state of the system leading water through the turbine, and is therefore given by the environment to the turbine,

- the actuator signal u is given by the turbine controller, and is therefore given by the environment of the turbine,

- the rotational speed $\dot{N}$ (or ω) is a state of the rotating aggregate, and is therefore given by the environment of the turbine, or rather to the part of the turbine converting pressure drop to mechanical energy.

It follows that the turbine itself determines the pressure drop Δp and the mechanical shaft power $\dot{W}_{\mathrm{s}}$. Thus, by knowing $\left(\dot{V}, u, \dot{N}\right)$, it must be possible to deduce $\left(\dot{W}, \Delta p\right)$.

The operation of the turbine will also depend on fluid properties such as density ρ, viscosity μ, and compressibility β (1/pressure):

$$\beta \triangleq \frac{1}{\rho}\frac{\partial\rho}{\partial p}, \tag{6.43}$$

as well as geometric properties such diameter D of the turbine rotor.

6.6.2   Mechanistic hydro turbine models

Turbine types   The two main *classes* of turbines are the impulse turbines and the reaction turbine. The most common *impulse turbine* is the *Pelton* turbine (1870s), while the two most common *reaction turbines* are the *Francis* turbine and the *Kaplan* turbine. Figure 6.12 gives a typical selection chart for hydro turbines depending on the relation between volumetric flow rate $\dot{V}$ ("Q" in the figure) and height difference between reservoir level and level downstream from the turbine ("H" in the figure) — the figure also includes a fourth turbine type, the Bulb turbine.

As seen from Fig. 6.12, the Pelton turbine is used for "small" flow rates $\dot{V}$ and pressure drops with equivalent water height of $[100, 2000]\,\mathrm{m}$. A needle is used to adjust a nozzle opening and thereby increasing the water velocity. High velocity water hits a bucket with two cups[23] and the energy is released as an impulse to atmospheric pressure, causing the wheel to rotate. A water flow deflector is used for additional and quick control of over-speed. See the paragraph on the Pelton turbine, p. 256, for details.

In reaction turbines, a rotor is forced to rotate by a high water flow rate, much like the propeller of a boat will rotate if the boat is towed. Two common types of reaction turbines are the Francis turbine (1848) and the Kaplan turbine (1912). The Francis turbine is used for medium to large flow rates $\dot{V}$ and waterfalls in the interval $[20, 500]\,\mathrm{m}$. Water enters through a spiral casing that surrounds the runner (rotor). The water enters the rotor through a ring of stationary guide vanes which direct the water flow onto the rotor blades at some optimal angle. After the turbine, the remaining kinetic energy is recovered in a draft tube of gradually increasing

---

[23]Pelton invented the use of two cups.
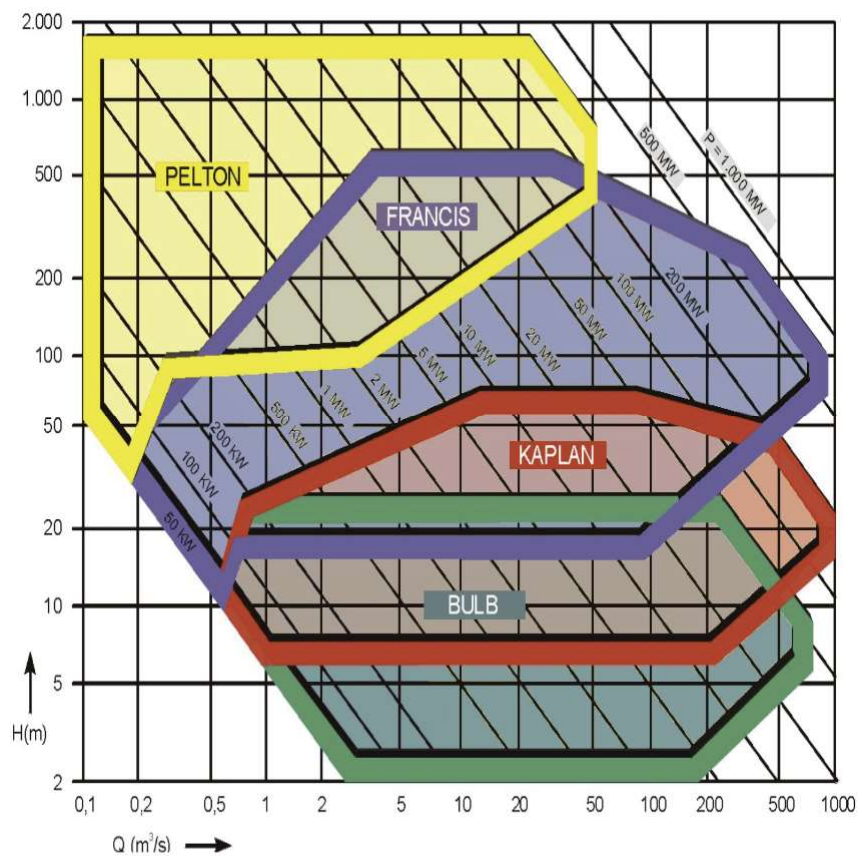
Figure 6.12: Turbine selection chart for selected turbine types. Due to Heinzmann HydroTech, India, see `http://www.heinzmann.co.in/technology.html`.

diameter, thereby gradually reducing the linear velocity and thus the kinetic energy towards zero. See the paragraph on the Francis turbine, p. 261, for details.

The Kaplan turbine is used for very large and varying flow rates $\dot{V}$ and low waterfalls in the range of $[7, 70]$ m; a typical use is in run-of-river hydro power production. In Kaplan turbines, water enters the runner radially through guide vanes, and the flow then changes to axial (vertical) flow where the axial propeller/turbine blades are rotated. The guide vanes are adjusted automatically for optimal operation, while the produced power is manipulated by changing the turbine blade pitch. See the paragraph on the Kaplan turbine, p. 269, for details.

Bulb turbines are used for very low water height differences, such as in tidal plants, etc.

Fundamental relations   Let the total energy be $E = K_a$ for the aggregate (rotating turbine and generator) and $\dot{E} = \dot{K} + \dot{P} \equiv 0$, this gives the aggregate energy balance (Eq. 6.11)

$$\frac{dK_a}{dt} = \underbrace{\dot{W}_i - \dot{W}_e - \dot{W}_{ff}}_{\triangleq \dot{W}_s} - \dot{W}_a$$

where $\dot{W}_s$ is the shaft work produced by the fluid (water) side, while $\dot{W}_a$ is the equivalent work on the aggregate side; $\dot{W}_a$ will include windage friction loss $\dot{W}_{fw}$, bearing friction loss $\dot{W}_{fb}$, friction loss in the generator $\dot{W}_{fg}$, etc., but also work on the aggregate due to consumption of electrical power $\dot{W}_e$ taken out from the generator:

$$\dot{W}_a = \dot{W}_{fw} + \dot{W}_{fb} + \dot{W}_{fg} + \dot{W}_e.$$

Here, we will focus on the shaft work $\dot{W}_s$ which consists of the net work due to forces from the fluid, $\Delta \dot{W}_E$, defined as

$$\Delta \dot{W}_E \triangleq \dot{W}_i - \dot{W}_e \qquad\qquad (6.44)$$

and possible fluid side friction drop through the turbine, $\dot{W}_{ff}$:

$$\dot{W}_s \triangleq \Delta \dot{W}_E - \dot{W}_{ff}.$$

When we have computed $\dot{W}_s$ (see below), the pressure drop Δp_s across the shaft of the fluid side can be computed from

$$\dot{W}_s = \Delta p_s \dot{V}$$

where $\dot{V}$ is the volumetric flow rate through the fluid side.

From Eq. 6.13

$$\dot{W}_i = T_i \omega = v_{\rho,i} \cdot \dot{m}_i v_i^t$$
$$\dot{W}_e = T_e \omega = v_{\rho,e} \cdot \dot{m}_e v_e^t$$

where $T = \dot{\mathcal{A}} = R\dot{\mathcal{M}}^t = R\dot{m}v^t$ and $v_\rho = \omega R$. We neglect the leakage of mass in the turbine, hence $\dot{m}_i = \dot{m}_e = \dot{m}$; we consider the case of constant density ρ, hence the volumetric flow rate through the fluid side is given by $\dot{m} = \rho \dot{V}$. Furthermore, the
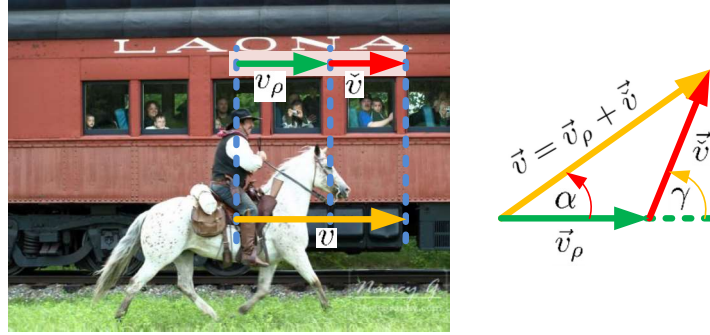
Figure 6.13: The absolute (earth bound) velocity v of a horse/rider is observed as a relative velocity $\check{v}$ by passengers in a train moving with a reference velocity v_ρ. More generally, an absolute velocity vector $\vec{v}$ is observed as relative velocity $\vec{\check{v}}$ for an observer moving with reference velocity $\vec{v}_\rho$; $\vec{v} = \vec{v}_\rho + \vec{\check{v}}$.

velocity v^{t} is the projection of the velocity tangential to the rotation (orthogonal to the radius r).

We thus have

$$\Delta\dot{W}_{\mathrm{E}} = \dot{m}\left(v_{\rho,\mathrm{i}} \cdot v_{\mathrm{i}}^{\mathrm{t}} - v_{\rho,\mathrm{e}} \cdot v_{\mathrm{e}}^{\mathrm{t}}\right) \tag{6.45}$$

where the "reference" velocity is $v_{\rho,j} \triangleq R_j\omega$; the expression for $\Delta\dot{W}_{\mathrm{E}}$ in Eq. 6.45 is known as *Euler's turbine equation*.

Turbine geometry*** (How much is general?)   In the development of models, absolute velocity v in an earth bound reference system will be essential, together with a reference velocity v_ρ in the same reference system, and a velocity $\check{v}$ relative to the reference velocity, Fig. 6.13.

Example 6.2. Absolute and relative velocity

If a horse/rider moves at velocity $v = 20\,\mathrm{km/h}$ in parallel to a train moving at reference velocity $v_\rho = 15\,\mathrm{km/h}$, the passengers of the train will perceive the cowboy to move at a velocity $\check{v} = v - v_\rho = 5\,\mathrm{km/h}$ relative to themselves.   ▲

For turbine models, we are interested in relating XXX

In general vector form, we relate absolute velocity (vector) $\vec{v}$ with reference velocity $\vec{v}_\rho$ and relative velocity $\vec{\check{v}}$ as follows,

$$\vec{v} = \vec{v}_\rho + \vec{\check{v}}.$$

If we decompose the vectors into an orthogonal coordinate system of x- and y-axes, and skip the vector symbol for the decomposed vectors, we get

$$v^x = v_\rho^x + \check{v}^x$$
$$v^y = v_\rho^y + \check{v}^y.$$

If we specifically choose $x \parallel \vec{v}_\rho$ and denote this by t ("tangential"), thus $y \perp \vec{v}_\rho$ denoted r ("radial"), we have $v_\rho^x = v_{\mathrm{r}}^{\mathrm{t}} = v_\rho$, and $v_\rho^y = v_{\mathrm{r}}^{\mathrm{r}} = 0$:

$$v^{\mathrm{t}} = v_\rho + \check{v}^{\mathrm{t}} \tag{6.46}$$
$$v^{\mathrm{r}} = \check{v}^{\mathrm{r}}. \tag{6.47}$$

Here,

$$v^{\mathrm{t}} = v \cdot \cos\alpha \tag{6.48}$$

$$\check{v}^{\mathrm{t}} = \check{v} \cdot \cos\gamma \tag{6.49}$$

$$v^{\mathrm{r}} = v \cdot \sin\alpha \tag{6.50}$$

$$\check{v}^{\mathrm{r}} = \check{v} \cdot \sin\gamma, \tag{6.51}$$

where it follows that

$$v^{\mathrm{t}} = v^{\mathrm{r}}\cot\alpha. \tag{6.52}$$

Furthermore, from the sine law, we have

$$\frac{v}{\sin(\pi - \gamma)} = \frac{v}{\sin\gamma} = \frac{\check{v}}{\sin\alpha}. \tag{6.53}$$

By combining Eq. 6.46 with Eqs. 6.48 and 6.49 to get

$$v \cdot \cos\alpha = v_\rho + \check{v} \cdot \cos\gamma, \tag{6.54}$$

we can use Eq. 6.53 to express $\check{v}$, and the relative velocity can be eliminated from Eq.6.54 to get

$$v \cdot \cos\alpha = v_\rho + \frac{\sin\alpha}{\sin\gamma} v \cdot \cos\gamma$$

$$\Downarrow$$

$$v_\rho = \frac{\cos\alpha \cdot \sin\gamma - \sin\alpha \cdot \cos\gamma}{\sin\gamma} v. \tag{6.55}$$

This expression relates the reference velocity v_ρ the absolute velocity v and the involved angles.

Here, we can alternatively use Eq. 6.50 and relate v_ρ to v^{r}:

$$v_\rho = \frac{\cos\alpha \cdot \sin\gamma - \sin\alpha \cdot \cos\gamma}{\sin\gamma} \frac{v^{\mathrm{r}}}{\sin\alpha}$$

$$\Downarrow$$

$$v_\rho = (\cot\alpha - \cot\gamma)v^{\mathrm{r}}. \tag{6.56}$$

The Pelton turbine: impulse transfer

Overview   The impulse turbine is a conceptually simple type of turbine, where the Pelton turbine is the most commonly used one today. Figure 6.14 illustrates the main concepts.

The impulse turbine consists of a nozzle ("0"–"1") where a needle in position Y can be moved to change the cross sectional area at position "1", and thus the velocity v_2. Then water from position "1" hits the buckets of the turbine wheel at position "2" and transfers energy to the rotating engine. It is natural to divide the treatment into one model for the nozzle, and another one for the bucket system/rotating engine.

In general, the mass flow rate $\dot{m}$ is assumed to be constant through the impulse turbine, i.e., in all position. Furthermore, we neglect compressibility of water which leads to a constant density ρ, hence the volumetric flow rate $\dot{V}$ is constant through the turbine.
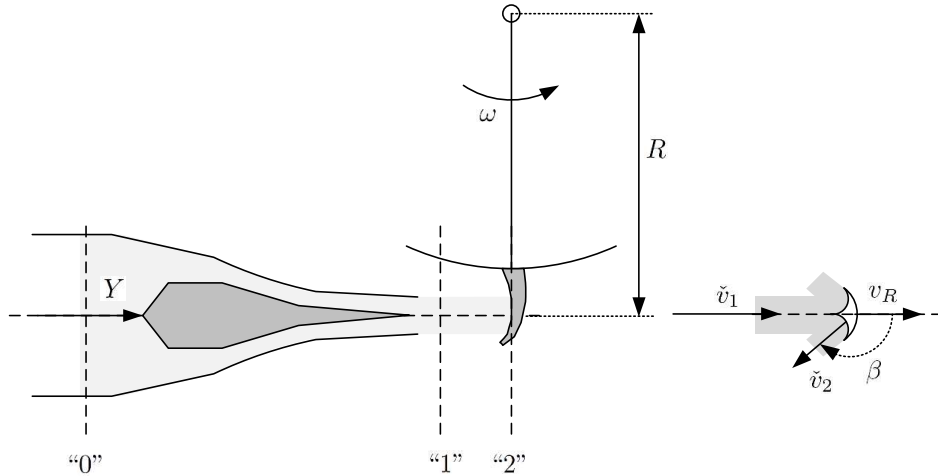
Figure 6.14: Some key concepts of the impulse turbine.

Nozzle pressure drop The nozzle model is based on a steady state energy balance. Thus the energy flow is the same at positions "0" and "1". Assuming a small nozzle, we can neglect potential energy and only include kinetic energy flow $\dot{K}$ and pressure-flow power $\dot{W}$, as well as friction loss $\dot{W}_\mathrm{f}$. Hence

$$\dot{K}_0 + \dot{W}_0 = \dot{K}_1 + \dot{W}_1 + \dot{W}_\mathrm{f}$$

where

$$\dot{K} = \frac{1}{2}\dot{m}v^2$$
$$\dot{W} = p\dot{V}.$$

With constant $\dot{m}$ and V, and $v = \dot{V}/A$, this leads to

$$\frac{1}{2}\dot{m}\left(\frac{\dot{V}}{A_0}\right)^2 + p_0\dot{V} = \frac{1}{2}\dot{m}\left(\frac{\dot{V}}{A_1}\right)^2 + p_1\dot{V} + \dot{W}_\mathrm{f}$$

$$\Downarrow$$

$$(p_0 - p_1)\,\dot{V} = \frac{1}{2}\dot{m}\dot{V}^2\left(\frac{1}{A_1^2} - \frac{1}{A_0^2}\right) + \dot{W}_\mathrm{f}.$$

Here, $\Delta p_\mathrm{n} \triangleq p_0 - p_1$ is the pressure drop across the nozzle. It is common to assume that $\dot{W}_\mathrm{f} \propto \dot{V}^2$, e.g.,

$$\dot{W}_\mathrm{f} = \frac{1}{2}\rho k_\mathrm{f}\dot{V}^2.$$

Finally, A_1 is a function of needle position Y; $A_1 = A_1(Y)$. Thus

$$\Delta p_\mathrm{n}\dot{V} = \frac{1}{2}\dot{V}^2\left[\dot{m}\left(\frac{1}{A_1^2(Y)} - \frac{1}{A_0^2}\right) + \rho k_\mathrm{f}\right].$$

By utilizing that $m = \rho \dot{V}$, we can alternatively find

$$\Delta p_{\mathrm{n}} \dot{V} = \frac{1}{2} \rho \dot{V}^2 \left[\dot{V} \left(\frac{1}{A_1^2 \left(Y \right)} - \frac{1}{A_0^2} \right) + k_{\mathrm{f}} \right]$$

and

$$\Delta p_{\mathrm{n}} = \frac{1}{2} \rho \dot{V} \left[\dot{V} \left(\frac{1}{A_1^2 \left(Y \right)} - \frac{1}{A_0^2} \right) + k_{\mathrm{f}} \right].$$

Geometry   The ideal transfer of power $\dot{W}_{\mathrm{t}}$ to the rotor of the turbo machine is given by Euler's turbine equation

$$\dot{W}_{\mathrm{t}} = \left(T_1 - T_2 \right) \omega$$

where T_1 is the torque at position "1" (or rather: when the water hits the bucket) and T_2 is the torque at position "2" (or rather for the water reflected from the bucket). In the Pelton turbine, the torques share the same radius R of the turbine wheel in Fig. 6.14:

$$T_1 = \dot{m} v_1^{\mathrm{t}} R$$
$$T_2 = \dot{m} v_2^{\mathrm{t}} R;$$

v_j^{t} indicates the tangential coordinate of the velocity in position j — parallel to $\dot{m}$; R is the radius of rotor where the mass hits the bucket, and we have utilized that the mass flow $\dot{m}$ is constant in size through the turbine. This also means that the reference velocity is the same for poth position "1" and position "2": $v_{\rho,1} = v_{\rho,2} = v_{\mathrm{R}} = \omega R$.

For position "1", we simply have that

$$v_1^{\mathrm{t}} = v_1 = \frac{\dot{V}}{A_1}.$$

For position "2", we observe from Fig. 6.14 that the *relative* velocity $\check{v}_2$ is reflected from the bucket at an angle β backwards. By relative velocity, we mean the velocity that we would observe had we been sitting and moving around on the turbine wheel. But the velocity we need in our expression for the torque, is the *absolute* velocity in the earth-bound coordinate system. Thus we need to find an expression for v_2^{t}.

First, we assume that the reflected relative velocity $\check{v}_2$ is proportional in size to the inlet relative velocity $\check{v}_1$:

$$\check{v}_2 = k \check{v}_1;$$

here $k \leq 1$ is some friction factor, typically $k \in [0.8, 0.9]$. Next, we need to relate the relative velocities to the absolute tangential velocity. Then we have

$$\check{v}_1 = v_1^{\mathrm{t}} - v_R = v_1 - v_R$$

and

$$v_2^{\mathrm{t}} = v_R - \check{v}_2 \cos \left(180 - \beta \right) = v_R + \check{v}_2 \cos \beta.$$

Here, a typical value for the reflection angle is $\beta = 165°$. We find

$$v_2^t = v_R + k \left(v_1 - v_R \right) \cos \beta.$$

The ideal turbine work thus becomes

$$\dot{W}_t = \left(T_1 - T_2 \right) \omega$$
$$\Downarrow$$
$$\dot{W}_t = \dot{m} \left(v_1^t - v_2^t \right) R\omega.$$

We have

$$v_1^t - v_2^t = v_1 - \left[v_R + k \left(v_1 - v_R \right) \cos \beta \right]$$
$$\Downarrow$$
$$v_1^t - v_2^t = \left(v_1 - v_R \right) \left(1 - k \cos \beta \right).$$

Shaft power   The ideally transferred power can then be written as

$$\dot{W}_t = \dot{m} v_R \left(v_1 - v_R \right) \left(1 - k \cos \beta \right).$$

It is of interest to see how we can maximize the performance of the turbine. Although the reference velocity v_R is given since $v_R = R\omega$ and ω normally is constrained by the grid frequency, let us consider the case when v_1 is known and we can vary v_R. To this end, the transferred power $\dot{W}_t \left(v_R \right)$ is maximised when $\frac{\partial \dot{W}_t}{\partial v_R} = 0$, leading to $\left(v_R \right)_{\max} = \frac{1}{2} v_1$ or

$$\dot{W}_t \left(v_R \right)_{\max} = \dot{m} \frac{v_1^2}{4} \left(1 - k \cos \beta \right).$$

Similarly, the maximal torque is given from $\dot{W} = T\omega = T \frac{v_R}{R} = T \frac{v_1}{2R}$, or

$$T_t \left(v_R \right)_{\max} = \dot{m} R \frac{v_1}{2} \left(1 - k \cos \beta \right).$$

The real shaft power transferred is the ideal power given by Euler's equation reduced by friction loss,

$$\dot{W}_s = \dot{W}_t - \dot{W}_{ft},$$

where for the case that $\dot{W}_{ft} \equiv 0$, $\dot{W}_s = \dot{W}_t$. Similarly, the real shaft torque $T_s \omega = \dot{W}_s$. Figure 6.15 illustrates how the friction free model $\dot{W}_s \left(v_R \right)$ fits with experimental data.

Possible explanations for the mismatch between the theoretical model and the actual data in Fig. 6.15 could be friction loss, the fact that there is not a continuum of buckets, etc. A common way to represent this mismatch is to say that there is a power loss proportional to $\dot{m} v_R^2$, thus

$$\dot{W}_{ft} = K' \dot{m} v_R^2 = K \left(1 - k \cos \beta \right) \dot{m} v_R^2,$$

leading to the shaft power

$$\dot{W}_s = \dot{m} v_R \left[v_1 - \left(1 + K \right) v_R \right] \left(1 - k \cos \beta \right).$$

$$T_s\,(v_R)_{\max} = \dot{m}R\frac{v_1}{2}\left(1 - k\cos\beta\right) \qquad \dot{W}_s\,(v_R)_{\max} \;=\; \dot{m}\frac{v_1^2}{4}\left(1 - k\cos\beta\right)$$
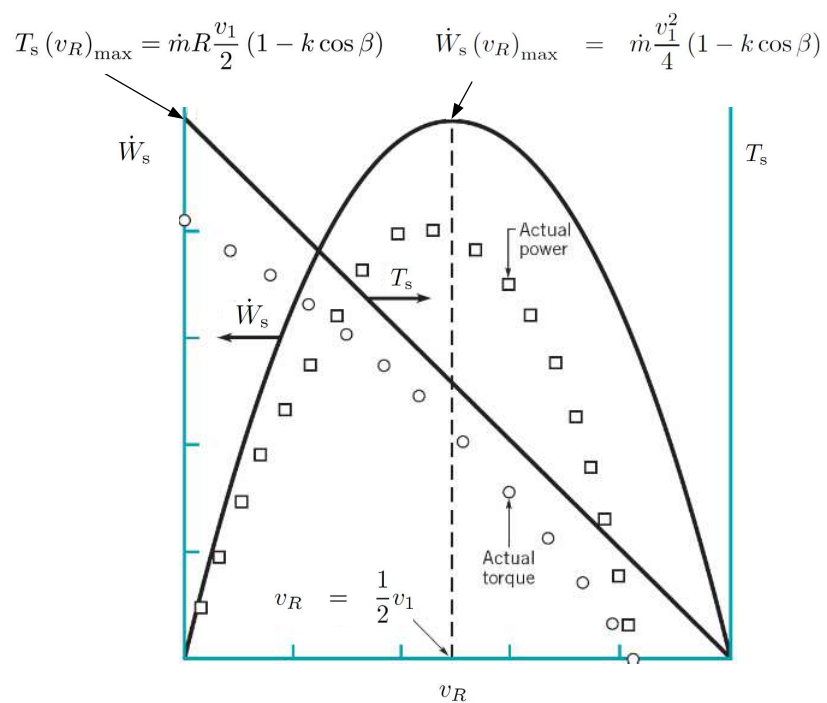

Figure 6.15: Comparison of how $\dot{W}_w$ fits with actual data. Taken from Jyn-Cherng Shieh (2007), `www.taiwan921.lib.ntu.edu.tw/mypdf/fluid12.pdf`, but with modified notation and correction of a typo in the expression for T_s.

It is easily found that $\dot{W}_s$ attains it maximum for v_R given by $(v_R)_{max} = \frac{1}{2(1+K)}v_1$ leading to

$$\dot{W}_s \left(v_R\right)_{max} = \dot{m}\frac{v_1^2}{4}\left(1 - k\cos\beta\right)\frac{1}{1+K}.$$

From Fig. 6.15, we see that in that figure,

$$\frac{1}{1+K} \approx 0.8 \Rightarrow K \approx \frac{1-0.8}{0.8} = 0.25.$$

Furthermore, from the expression for $\dot{W}_s$, we see that $\dot{W}_s = 0$ when $v_R = 0 \vee v_R = \frac{1}{1+K}v_1 = 0.8v_1$, which also fits well with Fig. 6.15.

In practical installations, there will be a deflector mechanism to reduce the velocity $v_1\delta\left(u_\delta\right)$ to avoid over-speed. A final expression for the shaft work could thus be

$$\dot{W}_s = \dot{m}v_R\left[\delta\left(u_\delta\right) \cdot v_1 - (1+K)v_R\right]\left(1 - k\cos\beta\right).$$

Model summary   Produced shaft power is given as

$$\dot{W}_s = \dot{m}v_R\left[\delta\left(u_\delta\right) \cdot v_1 - (1+K)v_R\right]\left(1 - k\cos\beta\right).$$

If needed, we can compute the pressure drop across the turbine itself from $\dot{W}_s = \Delta p_s\dot{V}$ where $\dot{V} = A_1\left(Y\right)v_1$.

The Francis turbine: reaction transfer

Overview   The Francis turbine is a radial flow turbine, and is illustrated in Fig. 6.16.

Figure 6.17 shows how the so-called guide vanes affect the flow of water towards the turbine stator.

In Fig. 6.17, the spiralling cage is designed so that the flow through each of N opening pairs of guide vanes is (approximately) the same, $\frac{\dot{V}}{N}$;[24] the linear velocity v_1 is also the same through each opening. The distance between each suspension point for guide vanes is d, each guide vane has the same angle α_1 with the vane perimeter, and the distance between each (almost) parallel guide vane is δ. It follows that d and δ are related as

$$\sin\alpha_1 = \frac{\delta}{d}.$$

With width w of the rotor and stator, it follows that the cross sectional area of the flow through each guide vane pair is $a_v = \delta \cdot w$, hence the linear velocity v_1 is related to $\dot{V}$ and α_1 as

$$v_1 = \frac{\dot{V}/N}{a_v} = \frac{\dot{V}/N}{\delta \cdot w} = \frac{\dot{V}/N}{\sin\alpha_1 \cdot d \cdot w} = \frac{\dot{V}}{Nd \cdot w \cdot \sin\alpha_1}.$$

---

[24]In the figure, only 3 openings are shown; the N openings are spread equidistantly around the stator entrance.
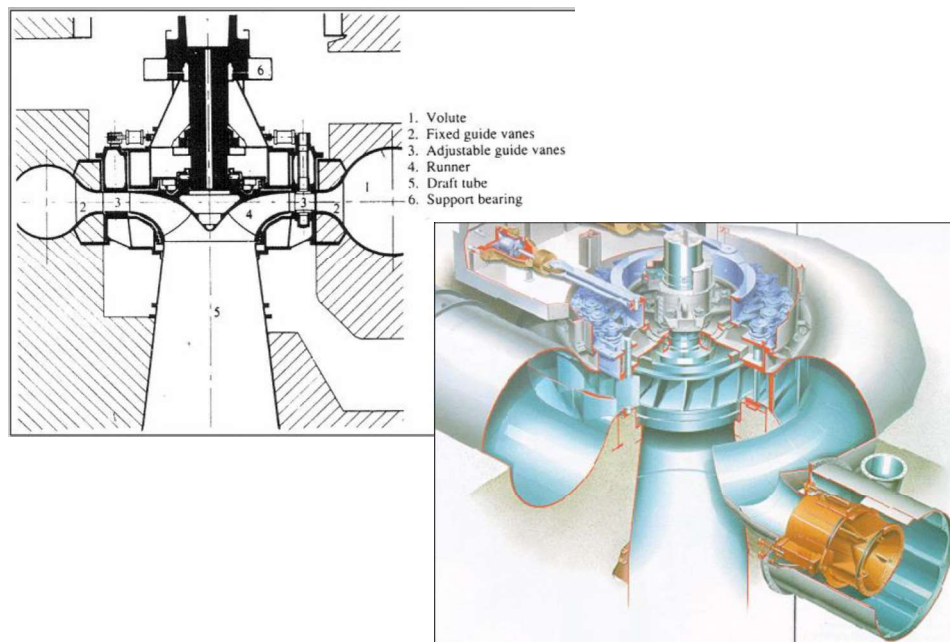
Figure 6.16: Principle drawing and illustration of Francis turbine. From Harinaldi, `http://staff.ui.ac.id/system/files/users/harinaldi.d/material/fluidsystem09-reactionturbine-francisandkaplan.pdf`.
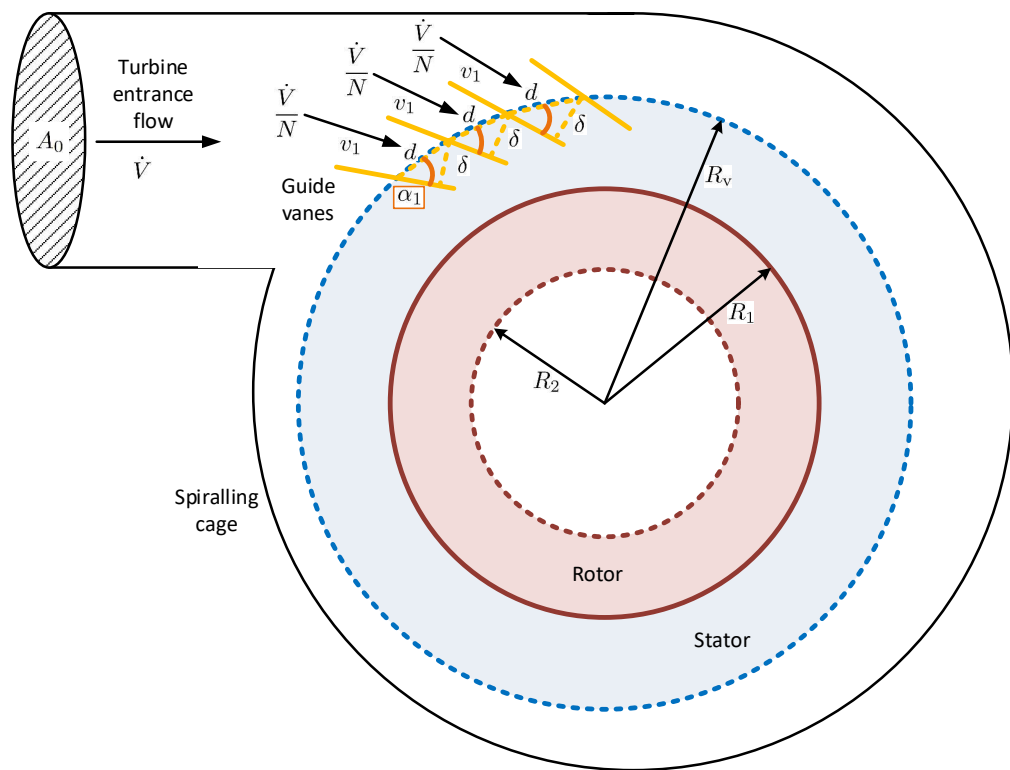

Figure 6.17: Effect of guide vane angle α_1 on stator inlet velocity v_1.

Here, $\wp_{\mathrm{v}} \triangleq Nd$ is the perimeter of the guide vane suspension circle, hence $Nd \cdot w = \wp_{\mathrm{v}} w = 2\pi R_{\mathrm{v}} w = A_{\mathrm{v}}$ is the maximal area opening through the guide vanes;

$$v_1 = \frac{\dot{V}}{A_{\mathrm{v}} \sin \alpha_1}.$$

The flow from the turbine entrance (volumetric flow rate $\dot{V}$, cross sectional area A_0) through the guide vanes and to the stator/rotor interface (volumetric flow rate $\dot{V}$, cross sectional area $A_{\mathrm{v}} \sin \alpha_1$) gives a certain pressure change. Simultaneously, the guide vanes steer the water at a certain angle α_1 towards the rotor blades, thus driving the rotor and producing a rotational power with another pressure drop through the rotor and to the exit from the rotor.

In the sequel, we first discuss the pressure drop across the guide vanes. Next, the rotational shaft power produced in the turbine is discussed. Finally, paragraph *Guide vane geometry* on p. 267 discusses how the actuator signal u relates to guide vane angle α_1.

Guide vane pressure drop We will assume that the flow from the turbine entrance through the inlet guide vanes follows Bernoulli's law. To this end, we have the following steady energy balance along stream lines, where we neglect any vertical difference in position:

$$\dot{K}_0 + p_0 \dot{V} = \dot{K}_1 + p_1 \dot{V} + \dot{W}_{\mathrm{fv}};$$

here subscript 0 indicates entrance to the turbine and subscript 1 indicates after guide vanes, while $\dot{W}_{\mathrm{fv}}$ is friction loss from turbine entrance and across guide vanes. Here, we have used that mass is not accumulated and assumed constant density, hence the volumetric flow rate is the same everywhere. From Fig. 6.17 and the above discussion, we have

$$\dot{K}_0 = \frac{1}{2} \dot{m} v_0^2 = \frac{1}{2} \dot{m} \frac{\dot{V}^2}{A_0^2}$$

$$\dot{K}_1 = \frac{1}{2} \dot{m} v_1^2 = \frac{1}{2} \dot{m} \frac{\dot{V}^2}{A_{\mathrm{v}}^2 \sin^2 \alpha_1}.$$

With $\dot{V} = \dot{m}/\rho$, we then have

$$\frac{1}{2} \dot{m} \frac{\dot{V}^2}{A_0^2} + p_0 \frac{\dot{m}}{\rho} = \frac{1}{2} \dot{m} \frac{\dot{V}^2}{A_{\mathrm{v}}^2 \sin^2 \alpha_1} + p_1 \frac{\dot{m}}{\rho} + \dot{W}_{\mathrm{fv}}.$$

Introducing

$$\Delta p_{\mathrm{v}} \triangleq p_0 - p_1,$$

we find

$$\Delta p_{\mathrm{v}} = \frac{\rho}{2} \left(\frac{1}{A_{\mathrm{v}}^2 \sin^2 \alpha_1} - \frac{1}{A_0^2} \right) \dot{V}^2 + \frac{\dot{W}_{\mathrm{fv}}}{\dot{V}}.$$

When the vanes are closing, $\alpha_1 \to 0$ and thus $\sin \alpha_1 \to 0$, the velocity $v_1 \propto \frac{1}{\sin \alpha_1}$ will go to infinity. However, Δp_{v} will go to infinity quadratically (hence, much faster),
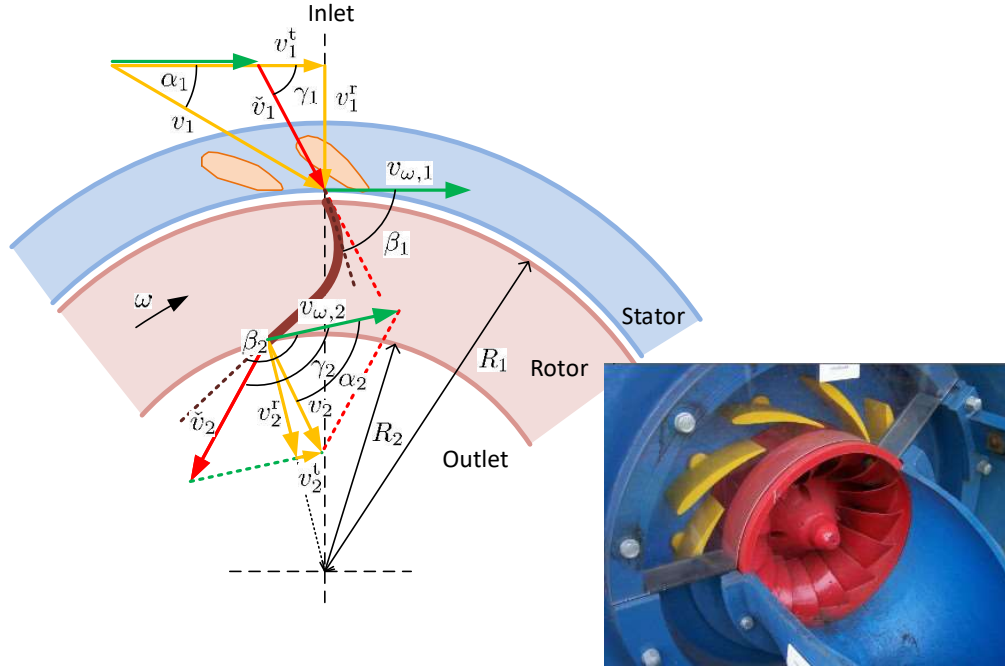
Figure 6.18: Key quantities in the Francis turbine model, with blade angles β_1 and β_2. The water effluent comes out from the paper plane.

and thus the counter pressure to the turbine entrance flow will block the flow of water as the guide vanes close.

In general, the *friction* loss will depend on (i) the mass flow rate, and (ii) the vane angle α_1. If we *simplify* the description and set $\dot{W}_{\mathrm{fv}} = \frac{k_{\mathrm{fv}}}{2}\dot{m}$, then

$$\Delta p_{\mathrm{v}} = \frac{1}{2}\rho \dot{V}_{\mathrm{p}} \left[\frac{A_0^2 - A_{\mathrm{v}}^2 \sin^2 \alpha_1}{A_0^2 A_{\mathrm{v}}^2 \sin^2 \alpha_1} + k_{\mathrm{fv}} \right].$$

As indicated above, the angle will be a function of the the actuator signal u.

From this discussion, we see that Δp_{v} may be either positive or negative, depending on the angle α_1 and the size of k_{fv}. In standard presentations of the Francis turbine, the pressure drop Δp_{v} is not discussed, and is thus implicitly neglected, or may alternatively be included in some overall efficiency of the turbine.

Geometry**   Insert??

Shaft power   Figure 6.18 shows absolute velocities, rotor reference velocities, and relative velocities in the Francis turbine.

We have seen that the shaft power $\dot{W}_{\mathrm{s}}$ produced in a turbo machine can be written as in Eq. 6.44,

$$\dot{W}_{\mathrm{s}} = \Delta \dot{W}_{\mathrm{t}} - \dot{W}_{\mathrm{ft}}$$

where the the change in work rate across the rotor is given in Eq. 6.45 and can be written as follows for the Francis turbine:

$$\Delta \dot{W}_t = \dot{m} \left(v_{\rho,1} v_1^t - v_{\rho,2} v_2^t \right),$$

where the reference velocity is

$$v_{\rho,j} = \omega R_j.$$

Being a radial flow turbine, the water net flow is in the *radial* direction. With *no mass accumulated* in the turbine, we have

$$\dot{V} = A_1 v_1^r = A_2 v_2^r.$$

Here, A_j is the area through which the water flows, typically equal to the perimeter of the turbine, $\wp_j = 2\pi R_j$, multiplied by the width of the turbine/blades w_j: $A_j = \wp_j w_j$, possibly with the reduction of the area taken by guide vanes, etc., expressed through some factor κ_j. Thus

$$A_j = 2\pi R_j w_j \kappa_j.$$

Next, it is desirable that there is *no shock* when the water hits the turbine blades, which implies that the angles of the relative velocities γ_j must be aligned with the blade angles β_j; $\gamma_j \equiv \beta_j$. At the inlet, Eq. 6.56 gives

$$v_{\rho,1} = \left(\cot \alpha_1 - \cot \gamma_1 \right) v_1^r \tag{6.57}$$

where $v_{\rho,1} = \omega R_1$ is given by state ω, blade inlet angle β_1 given by design, $v_1^r = \frac{\dot{V}}{A_1}$ is given by state $\dot{V}$, and the inlet guide vane angle α_1 is given by control signal u. It follows that γ_1 is then constrained by the above equation, and we do not have the freedom to align γ_1 with the blade angle β_1: this alignment can only be done in a design phase — changing either of α_1, ω (through $v_{\rho,1}$) or $\dot{V}$ (through v_1^r) will change γ_1 accprdomg to Eq. 6.57 and make it differ from β_1. When operating with $\gamma_1 \neq \beta_1$, this leads to a friction-like hydraulic loss in the turbine.

For the outlet from the turbine, however, Eq. 6.56 can be achieved with $\gamma_2 = \beta_2$, leading to

$$v_{\rho,2} = \left(\cot \alpha_2 - \cot \beta_2 \right) v_2^r. \tag{6.58}$$

Here, reference velocity $v_{\rho,2} = \omega R_2$, blade outlet angle β_2 is given by design, and radial outlet velocity is $v_2^r = \frac{\dot{V}}{A_2}$. Thus, this equation gives the angle α_2.

From Eq. 6.52, we finally have the friction free shaft power as

$$\Delta \dot{W}_t = \dot{m} \left(v_{\rho,1} v_1^r \cot \alpha_1 - v_{\rho,2} v_2^r \cot \alpha_2 \right)$$

or with

$$v_2^r \cot \alpha_2 = v_{\rho,2} + v_2^r \cot \beta_2,$$

we find

$$\Delta \dot{W}_t = \dot{m} \left(v_{\rho,1} v_1^r \cot \alpha_1 - v_{\rho,2} \left(v_{\rho,2} + v_2^r \cot \beta_2 \right) \right)$$

$$\Downarrow$$

$$\Delta \dot{W}_t = \dot{m} \left(\omega R_1 \frac{\dot{V}}{A_1} \cot \alpha_1 - \omega R_2 \left(\omega R_2 + \frac{\dot{V}}{A_2} \cot \beta_2 \right) \right).$$

Here, $\alpha_1 \leq 90°$ is a function of the guide vane servo position u, and $\beta_2 \leq 90°$ is a design variable.

In turbine *design*, the following considerations are important:

1. For the *nominal* operating condition with given ω , $\dot{V}$, and operating guide vane angle α_1, a suitable turbine with R_1 , A_1, β_1, is selected such that the influent *no-shock condition* of Eq. 6.57 can be achieved with $\gamma_1 = \beta_1$. This will reduce the hydraulic friction loss.

   If the turbine is operated at conditions different from the nominal ones, this will incur a friction shock loss which, e.g., can be expressed as

$$\dot{W}_{\text{ft},1} = \mathcal{F}_{\text{ft},1} \left(\cot \gamma_1 - \cot \beta_1, \dot{V} \right) \geq 0$$

   where β_1 is a design variable (inlet blade angle) and $\cot \gamma_1$ is found from Eq. 6.57 as

$$\cot \gamma_1 = \cot \alpha_1 - \frac{v_{\rho,1}}{v_1^{\text{r}}} = \cot \alpha_1 - \frac{\omega R_1}{\dot{V}/A_1}.$$

   As an example, we could postulate ($\dot{V} \geq 0$)

$$\dot{W}_{\text{ft},1} = k_{\text{ft},1} \dot{V} \left(\cot \gamma_1 - \cot \beta_1 \right)^2 .$$

2. For the nominal operating condition with effluent no-shock condition Eq. 6.58 satisfied, the so-called *no-whirl effluent condition* $\alpha_2 = \frac{\pi}{2} \Rightarrow \cot \alpha_2 = 0$ is enforced, which increases and simplifies the shaft power to $\Delta \dot{W}_{\text{t}} = \dot{m} \omega R_1 \frac{\dot{V}}{A_1} \cot \alpha_1$.

   Effluent whirl both reduces the shaft power directly, and gives some hydraulic friction loss:

$$\dot{W}_{\text{ft},2} = \mathcal{F}_{\text{ft},2} \left(\cot \alpha_2, \dot{V} \right) \geq 0$$

   where

$$\cot \alpha_2 = \cot \beta_2 + \frac{\omega R_2}{\dot{V}/A_2}.$$

   As an example, we could postulate

$$\dot{W}_{\text{ft},2} = k_{\text{ft},2} \dot{V} \cot^2 \alpha_2.$$

Model summary   Produced shaft power is given as

$$\dot{W}_{\text{s}} = \Delta \dot{W}_{\text{t}} - \dot{W}_{\text{ft}}$$

where

$$\Delta \dot{W}_{\text{t}} = \dot{m} \omega \left(R_1 \frac{\dot{V}}{A_1} \cot \alpha_1 - R_2 \left(\omega R_2 + \frac{\dot{V}}{A_2} \cot \beta_2 \right) \right)$$

while, e.g.,

$$\dot{W}_{\text{ft}} = k_{\text{ft},1} \dot{V} \left(\cot \gamma_1 - \cot \beta_1 \right)^2 + k_{\text{ft},2} \dot{V} \cot^2 \alpha_2 + k_{\text{ft},3} \dot{V}^2$$
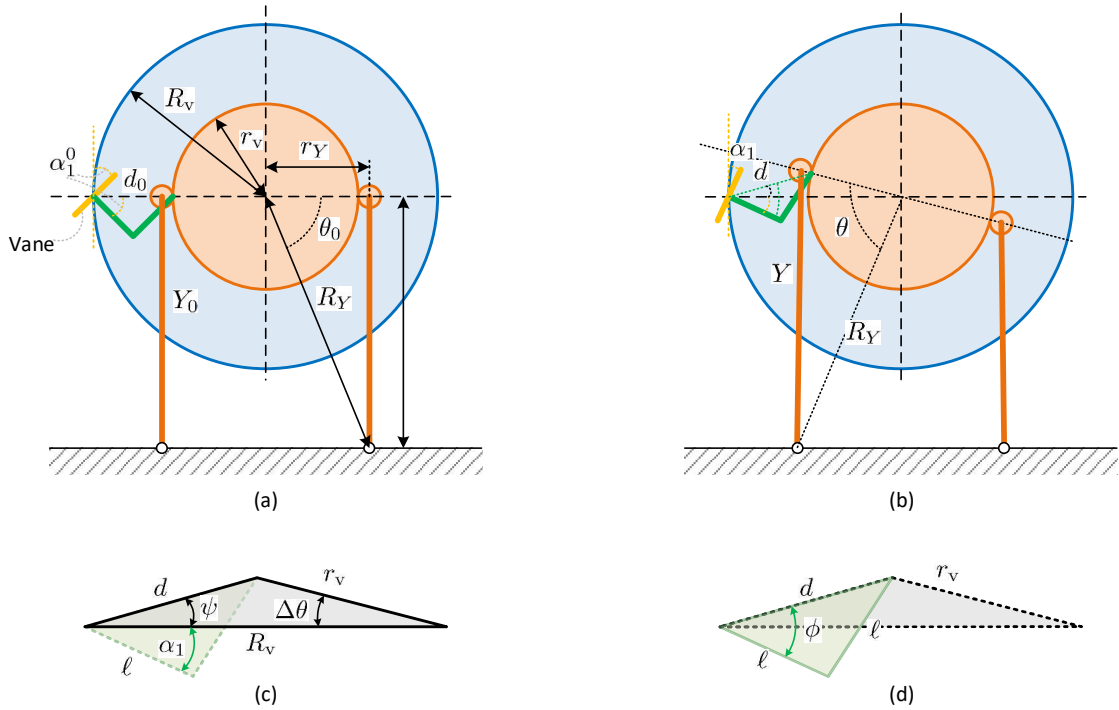
Figure 6.19: Guide vane geometry relating actuator position Y to guide vane angle α_1.

where $k_{\text{ft},3}$ gives some standard friction loss due to wall friction, etc. Here, $\dot{m}, \dot{V}$ will be a state of the entrance system ($\dot{m} = \rho \dot{V}$), ω will be a state of the aggregate, α_1 will be given by the actuator position u. The total work rate removed through the turbine will be

$$\dot{W}_{\text{t}} = \dot{W}_{\text{s}} + \Delta p_{\text{v}} \dot{V},$$

thus the total pressure loss Δp_{t} across the turbine can be found from $\dot{W}_{\text{t}} = \Delta p_{\text{t}} \dot{V}$.

Guide vane geometry The guide vane geometry is depicted in Fig. 6.19.[25]
From Fig. 6.19 (a), assuming that the actuator cylinder is "vertical" in position "0", we find that

$$R_Y^2 = r_Y^2 + Y_0^2$$
$$\cos \theta_0 = \frac{r_Y}{R_Y}.$$

Clearly, $d_0 = R_{\text{v}} - r_{\text{v}}$. Next, moving the actuator to position Y, Fig. 6.19 (b) with the cosine law gives

$$Y^2 = r_Y^2 + R_Y^2 - 2 r_Y R_Y \cos \theta,$$

---

[25]www.mekanizmalar.com/francis-turbine-wicket-gate-animation.html

Table 6.6: Example parameters for Guide Vane system.

Parameter	Value	Parameter	Value
r_v	$1.5\,\mathrm{m}$	r_Y	$1.6\,\mathrm{m}$
R_v	$2\,\mathrm{m}$	R_Y	$3\,\mathrm{m}$
ℓ	$1.8 \cdot \sqrt{\dfrac{(R_v - r_v)^2}{2}}$		

thus specifying angle θ. We introduce the change in angle θ as (Fig. 6.19 (b), (c)) as

$$\Delta\theta \equiv \theta - \theta_0.$$

Then, applying the cosine law to Fig. 6.19 (c) gives length d from[26]

$$d^2 = r_v^2 + R_v^2 - 2r_v R_v \cos\Delta\theta$$

and then angle ψ from

$$r_v^2 = d^2 + R_v^2 - 2d \cdot R_v \cos\psi;$$

here it is necessary to ensure that the sign of ψ equals the sign of $\Delta\theta$.

From Fig. 6.19 (d) and applying the cosine law, we find

$$\ell^2 = \ell^2 + d^2 - 2\ell d \cdot \cos\phi \Rightarrow \cos\phi = \frac{d}{2\ell}.$$

Finally, we find the guide vane angle as

$$\alpha_1 = \phi - \psi.$$

In the above development, it has been assumed that the guide vane is perpendicular to the attached "arm" of length ℓ, and that in position "0", a guide vane is at position "9 o'clock", Fig. 6.19 (a).

As a simple example, consider the guide vane parameters as in Table 6.6 — these numbers are not necessarily realistic.

The mapping from actuator position Y to guide vane angle α_1 can then be found as in the Python code below (file `guideVaneGeometry.py`).

```python
# -*- coding: utf-8 -*-
"""
Created on Tue Jan 17 16:02:20 2017

@author: Bernt Lie
"""
import numpy as np
import numpy.random as nr
import matplotlib.pyplot as plt
import pandas as pd
#
rv = 1.5
```

---

[26]Clearly, $d \in [d_0, 2\ell]$.

```
13  Rv = 2
14  rY = 1.6
15  RY = 3
16  #
17  Y0 = np.sqrt(RY**2-rY**2)
18  theta0 = np.arccos(rY/RY)
19  d0 = Rv-rv
20  #
21  L = np.sqrt(d0**2/2)*1.8
22  alpha10 = np.arccos(d0/(2*L))
23  #
24  Y = np.linspace(2.25,3.22)
25  #
26  theta = np.arccos((rY**2 + RY**2 - Y**2)/2/rY/RY)
27  dtheta = theta-theta0
28  d = np.sqrt(rv**2 + Rv**2-2*rv*Rv*np.cos(dtheta))
29  psi = np.arccos((d**2 + Rv**2 - rv**2)/(2*d*Rv))*np.sign(
        dtheta)
30  phi = np.arccos(d/2/L)
31  #
32  alpha1 = phi - psi
33  #
34  plt.plot(Y,alpha1*180/np.pi,linewidth=2.5)
35  plt.xlabel(r'$Y$␣[m]')
36  plt.ylabel(r'$\alpha_1$␣[${}^\circ$]')
37  plt.title(r'Guide␣Vane␣angle␣$\alpha_1$␣as␣a␣function␣of␣
        actuator␣position␣$Y$')
38  plt.grid(True)
39  plt.hold(True)
40  plt.plot(Y0,alpha10*180/np.pi,'ko')
41  plt.hold(False)
```

This case leads to the guide vane characteristic of Fig. 6.20.

The shape of the Guide Vane characteristic will depend on the chosen geometry, but with sensible geometry, it is possible to make the mapping from Y to α_1 fairly linear.

In order to change angle α_1, it is necessary to use a servo motor. Depending on how the control loop is constructed, it may be possible to specify the setpoint to angle α_1, a setpoint to $\sin\alpha_1$, or a setpoint to Y. The closed servo loop normally adds a time constant of about 1 s to the system.

The Kaplan turbine: reaction transfer

Overview The Kaplan turbine is an axial flow turbine, and is illustrated in Fig. 6.21.

Figure 6.22 shows some velocities in the Kaplan turbine.